

See discussions, stats, and author profiles for this publication at: <https://www.researchgate.net/publication/7106970>

Chiral Phosphoramidate-Catalyzed Aldol Additions of Ketone Trichlorosilyl Enolates. Mechanistic Aspects

ARTICLE *in* THE JOURNAL OF ORGANIC CHEMISTRY · JUNE 2006

Impact Factor: 4.72 · DOI: 10.1021/jo060243v · Source: PubMed

CITATIONS

49

READS

33

6 AUTHORS, INCLUDING:



Ken-Tsung Wong

National Taiwan University

261 PUBLICATIONS 7,940 CITATIONS

SEE PROFILE



Yutaka Nishigaichi

Shimane University

68 PUBLICATIONS 745 CITATIONS

SEE PROFILE

Chiral Phosphoramidate-Catalyzed Aldol Additions of Ketone Trichlorosilyl Enolates. Mechanistic Aspects

Scott E. Denmark,* Son M. Pham, Robert A. Stavenger, Xiping Su, Ken-Tsung Wong, and Yutaka Nishigaichi

Department of Chemistry, Roger Adams Laboratory, University of Illinois, Urbana, Illinois 61801

denmark@scs.uiuc.edu

Received February 6, 2006



The mechanism of the catalytic, enantioselective addition of trichlorosilyl enolates to aldehydes has been investigated. Kinetic studies using ReactIR and rapid injection NMR (RINMR) spectroscopy have confirmed the simultaneous operation of dual mechanistic pathways involving either one or two phosphoramidates bound to a siliconium ion organizational center. This mechanistic dichotomy was initially postulated on the basis of catalyst loading studies and nonlinear effects studies. This duality explains the difference in reactivity and stereoselectivity of various classes of phosphoramidates. Determination of Arrhenius activation parameters revealed that aldol addition occurs through the reversible albeit unfavorable formation of an activated complex, and natural-abundance ^{13}C NMR kinetic isotope effect (KIE) studies have determined that the turnover limiting step is the aldol addition. A thorough examination of a range of phosphoramidates has established empirical structure–activity selectivity relationships. In addition, the effects of catalyst loading, rate of addition, solvents, and additives have been studied and together allow the formulation of a unified mechanistic picture for the aldol addition.

Introduction and Background

In recent years, our laboratories have been actively engaged in the development of Lewis base catalyzed stereoselective reactions of organotrichlorosilanes.¹ The reactions promoted by these reagents are highly responsive to the action of chiral Lewis bases, enhancing both reactivity and stereoselectivity for a broad range of useful transformations including aldol additions,² allylations,³ and epoxide openings.⁴

Primary among these has been the development of enantioselective aldol additions catalyzed by chiral phosphoramidates. These endeavors have provided new avenues for the stereoselective addition of methyl and cyclic trichlorosilyl enolates

to a wide range of aryl and unsaturated aldehydes.⁵ A particularly important feature among substituted enolates in this reaction is the configurational correlation between enolate geometry and reaction diastereoselectivity. Using geometrically defined trichlorosilyl enolates of either *E*- or *Z*-configuration, both syn and anti products may be obtained through the selection of an appropriate phosphoramidate.⁶ More recently, we have expanded this field to encompass trichlorosilyl enolates bearing either α - and β -oxygen substituents with α - and β -stereogenic centers with excellent results.⁷ In all cases, high double diastereoselection is achieved with no deleterious influence from the resident heteroatom. Additional progress has been made in

(1) Denmark, S. E.; Fujimori, S. In *Modern Aldol Reactions*; Mahrwald, R., Ed.; Wiley-VCH: Weinheim, 2004; Vol. 2, Chapter 7.

(2) Denmark, S. E.; Stavenger, R. A. *Acc. Chem. Res.* **2000**, *33*, 432–440.

(3) (a) Denmark, S. E.; Fu, J.; Coe, D. M.; Su, X.; Pratt, N. E.; Griedel, B. D. *J. Org. Chem.* **2006**, *71*, 1513–1522. (b) Denmark, S. E.; Fu, J.; Lawler, M. J. *J. Org. Chem.* **2006**, *71*, 1523–1536. (c) Denmark, S. E.; Fu, J. *Chem. Commun.* **2003**, 167–170. (d) Denmark, S. E.; Fu, J. *J. Am. Chem. Soc.* **2000**, *122*, 12021–12022. (e) Denmark, S. E.; Fu, J. *J. Am. Chem. Soc.* **2001**, *123*, 9488–9489.

(4) Denmark, S. E.; Barsanti, P. A.; Wong, K.-T.; Stavenger, R. A. *J. Org. Chem.* **1998**, *63*, 2428–2429.

(5) (a) Denmark, S. E.; Stavenger, R. A.; Wong, K.-T.; Su, X. *J. Am. Chem. Soc.* **1999**, *121*, 4982–4991. (b) Denmark, S. E.; Stavenger, R. A. *J. Am. Chem. Soc.* **2000**, *122*, 8837–8847. (c) Denmark, S. E.; Stavenger, R. A.; Wong, K.-T. *Tetrahedron* **1998**, *54*, 10389–10402.

(6) (a) Denmark, S. E.; Su, X.; Nishigaichi, Y. *J. Am. Chem. Soc.* **1998**, *120*, 12990–12991. (b) Denmark, S. E.; Pham, S. M. *J. Org. Chem.* **2003**, *68*, 5045–5055.

(7) (a) Denmark, S. E.; Fujimori, S.; Pham, S. M. *J. Org. Chem.* **2005**, *70*, 10823–10840. (b) Denmark, S. E.; Fujimori, S. *Org. Lett.* **2002**, *4*, 3477–3480. (c) Denmark, S. E.; Fujimori, S. *Org. Lett.* **2002**, *4*, 3473–3476. (d) Denmark, S. E.; Fujimori, S. *Synlett* **2001**, 1024–1029. (e) Denmark, S. E.; Pham, S. M. *Org. Lett.* **2001**, *3*, 2201–2204. (f) Denmark, S. E.; Stavenger, R. A. *J. Org. Chem.* **1998**, *63*, 9524–9527.

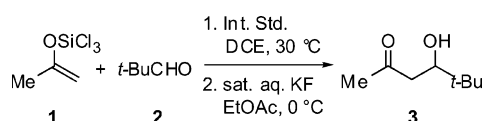
the field of crossed aldehyde–aldehyde aldol additions⁸ as well as acetate–ketone aldol additions.⁹

The conceptual framework for the design and implementation of the novel class of reactions has been described previously in a full account.¹ From its inception, the Lewis base catalysis concept was mechanistically unique among asymmetric transformations, and indeed, a number of papers disclosing critical kinetic¹⁰ spectroscopic¹¹ and mechanistic^{6a} insights have appeared. The objective of this full account is to present an integrated analysis of all the foregoing studies together with new structure/selectivity studies, medium effects and additional mechanistic studies and therefrom a unified mechanistic picture of the Lewis-base-catalyzed aldol addition reaction of trichlorosilyl enolates.

Results

1. Unpromoted Reactions. 1.1. Kinetic Studies. Initial kinetics studies were conducted with aliphatic aldehyde partners because of retro-aldolization of aromatic aldol adducts during gas chromatographic analysis. To further simplify the kinetic analysis, the use of an unsubstituted trichlorosilyl enolate eliminated the need to analyze mixtures of diastereomers. Following a brief survey, the combination of acetone derived trichlorosilyl enolate **1**¹² and pivalaldehyde (**2**) was selected for the initial kinetic runs, Scheme 1.^{10a} To accurately measure substrate concentrations during the course of the aldol addition, it was necessary to employ a nonvolatile, unreactive internal standard for which precise response factors could be determined. Adamantane fit the desired criteria and was used as the internal standard (Int. Std.) in all subsequent GC kinetic runs. An additional albeit minor deviation from the standard reaction conditions involved using 1,2-dichloroethane (DCE) as a reaction medium to allow for a larger temperature range which would be necessary for the determination of Arrhenius parameters.

SCHEME 1



The overall reaction order could be determined for the unpromoted reaction at 30 °C, by employing pseudo-order conditions. The reaction was shown to be first order in enolate, using 10 equiv of **2**, by virtue of a best fit analysis of first and second-order functions, Figure 1. Likewise, the reaction was determined to be first order in aldehyde using 10 equiv of **1**. Thus, the uncatalyzed aldol addition was determined to be second-order overall and first order in each component.

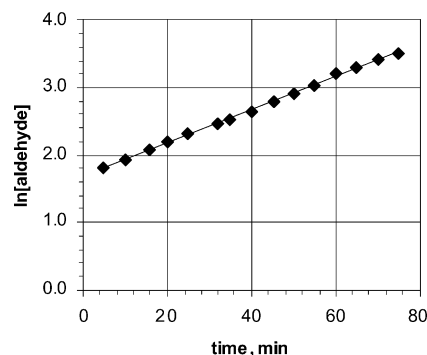


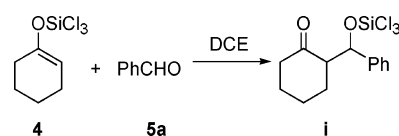
FIGURE 1. Plot of $\ln[\text{aldehyde}]$ versus time for the uncatalyzed addition of **1** to **2**. The graph depicts a linear fit, $f(x) = mx + b$ ($m = 0.025$, $R^2 = 0.999$), for a first-order reaction.

Determination of Arrhenius activation parameters was completed in the usual manner by measuring the rate constant of the uncatalyzed reaction as a function of temperature between 25 and 60 °C.¹³ Interestingly, analysis of the activation parameters (calculated for $T = 303$ K) reveals an unexpectedly large entropic contribution ($\Delta S^\ddagger = -56.7 \pm <0.1$ cal mol⁻¹ K⁻¹) to the free energy of activation ($\Delta G^\ddagger = 23.0 \pm <0.1$ kcal mol⁻¹). Although a large entropic contribution suggests a highly ordered transition structure, its magnitude does not preclude an unfavorable preequilibrium binding between the trichlorosilyl enolate and aldehyde prior to aldolization. The relatively small value for the enthalpy of activation ($\Delta H^\ddagger = 5.8 \pm <0.1$ kcal mol⁻¹) illustrates the extreme reactivity of trichlorosilyl enolates.

Although kinetic analysis by aliquot sampling is reliable for reactions run at or above room temperature, it is generally unsuitable for fast reactions performed at subambient temperatures. With this in mind, kinetic analysis of catalyzed reactions was determined by in situ monitoring using IR spectroscopy.

The kinetic analysis described above was confirmed using a Mettler-Toledo ReactIR¹⁴ for the acetone enolate/pivalaldehyde system without adamantane. Gratifyingly, the kinetic results from IR analysis were in excellent agreement with those from GC analysis,^{10a} and we could next turn our attention to the aldol system of the cyclohexanone-derived trichlorosilyl enolate **4**¹² and benzaldehyde (**5a**), Scheme 2. Although kinetic analysis from the rates of formation of diastereomers of **i** remained a concern, the spectroscopic coincidence of the syn and anti diastereomers removed this complication.

SCHEME 2



The Arrhenius parameters were again determined for the uncatalyzed addition of cyclohexanone trichlorosilyl enolate **4** to benzaldehyde using in situ IR monitoring (calculated for $T = 303$ K). Again, the activation parameters reveal a large entropic contribution ($\Delta S^\ddagger = -58.2 \pm 1.6$ cal mol⁻¹ K⁻¹) and a small enthalpic contribution ($\Delta H^\ddagger = 2.4 \pm 0.5$ kcal mol⁻¹) to the free

(8) (a) Denmark, S. E.; Ghosh, S. K. *Angew. Chem., Int. Ed.* **2001**, *40*, 4759–4762. (b) Denmark, S. E.; Bui, T. *Proc. Nat. Acad. Sci. U.S.A.* **2004**, *101*, 5439–5444. (c) Denmark, S. E.; Bui, T. *J. Org. Chem.*, **2005**, *70*, 10393–10399.

(9) (a) Denmark, S. E.; Winter, S. B. D.; Su, X.; Wong, K.-T. *J. Am. Chem. Soc.* **1996**, *118*, 7404–7405. (b) Denmark, S. E.; Fan, Y. *J. Am. Chem. Soc.* **2002**, *124*, 4233–4235. (c) Denmark, S. E.; Fan, Y.; Eastgate, M. D. *J. Org. Chem.* **2005**, *70*, 5235–5248.

(10) (a) Denmark, S. E.; Pham, S. M. *Helv. Chim. Acta* **2000**, *83*, 1846–1853. (b) Pham, S. M. Ph.D. Thesis, University of Illinois at Urbana–Champaign, 2002.

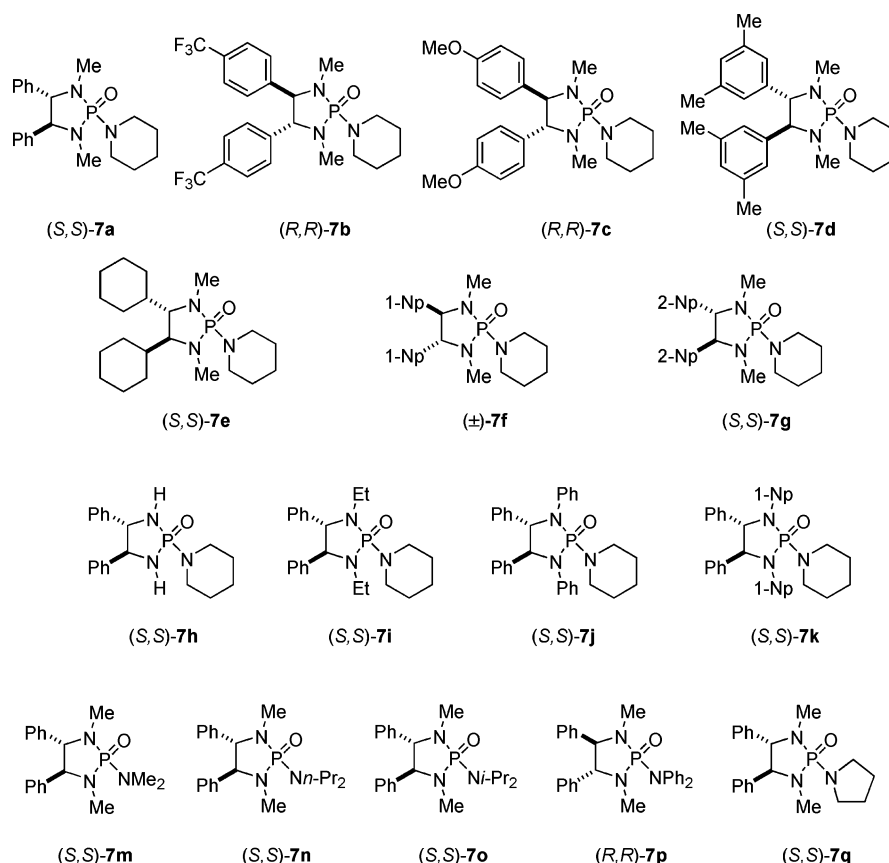
(11) (a) Denmark, S. E.; Su, X. *Tetrahedron* **1999**, *55*, 8727–8738. (b) Denmark, S. E.; Fu, J. *J. Am. Chem. Soc.* **2003**, *125*, 2208–2216.

(12) Denmark, S. E.; Stavenger, R. A.; Winter, S. B. D.; Wong, K.-T.; Barsanti, P. A. *J. Org. Chem.* **1998**, *63*, 9517–9523.

(13) All kinetic runs were performed in triplicate to ensure accuracy and reproducibility. See the Supporting Information for complete details.

(14) ReactIR 1000 fitted with a 5/8 in. DiComp Probe, running software version 2.1a. Mettler-Toledo AutoChem Inc., 7075 Samuel Morse Dr., Columbia, MD, 21046, or visit <http://us.mt.com>.

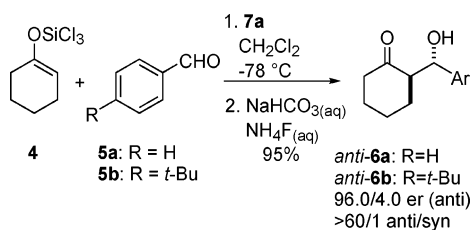
CHART 1



energy of activation ($\Delta G^\ddagger = 20.0 \pm 1.0 \text{ kcal mol}^{-1}$). Compared with the acetone–pivalaldehyde example, ΔG^\ddagger is smaller for addition of cyclohexanone enolate to benzaldehyde and in agreement with our preparative examples which demonstrate that additions to hindered aliphatic aldehydes such as pivalaldehyde are slower with respect to additions to benzaldehyde.

1.2. Background Reactions at -78°C . To assess the efficiency of phosphoramidates in promoting the aldol reactions, a control reaction without promoters needed to be performed. Although trichlorosilyl enolate **4** did not react with 1-naphthaldehyde at -78°C (96% recovery of 1-naphthaldehyde was obtained after 2 h), the reaction between **4** and **5a** or **5b** resulted appreciable amount of products syn-**6a** and syn-**6b**. For example, after 2 h at -78°C , both **5a** and **5b** gave 19% of the isolated syn products **6a** and **6b**, and the aldehyde **5b** was recovered in 78% yield. When the reactions were quenched after 8 min at -78°C , only 2% conversion had occurred for both **5a** and **5b** as judged by ^1H NMR. On the other hand, the promoted reactions were very fast. Using 10 mol % of chiral phosphoramidate **7a**, Chart 1, the reaction was complete within 8 min at -78°C , Scheme 3. Even quenching the reaction after 10 s resulted in a greater than 50% conversion.

SCHEME 3



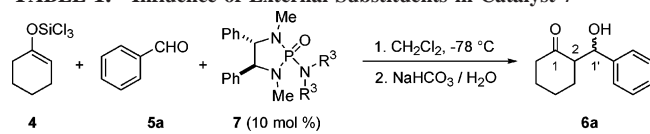
2. Promoted Reactions. 2.1. Survey of Chiral Phosphoramidates.

2.1.1. Reaction with Cyclohexanone-Derived Enolate **4.** Initial studies with cyclohexanone-derived enolate **4** showed that *N,N'*-dimethylstilbene-1,2-diamine derived phosphoramidate **7a** is the best catalyst for the aldol reactions.⁵ To understand the structural features that are important for rate as well as selectivity and to further optimize the structure of this catalyst, we undertook a survey of relevant phosphoramidate structures around the basic skeleton of **7a** (Chart 1). The phosphoramidates shown in Chart 1 were all prepared in enantiomerically pure form as has been described previously.¹⁵

2.1.1.1. Survey of External Substituents. Although it had been established early on that the piperidinyl group is critical for high stereoselectivities, the ease with which catalysts bearing modifications on the external nitrogen can be prepared allowed us to readily examine the effects of these peripheral modifications. The results are listed in Table 1.

All of the phosphoramidates **7m** through **7q** effectively catalyzed the reaction to give good yields of aldol products, however both the diastereo- and the enantioselectivities varied dramatically. Whereas **7a** was highly anti diastereoselective, **7m** and **7q** were less so (Table 1, entries 1 and 5) and **7p** was only slightly anti selective (Table 3, entry 4). On the other hand with **7n** and **7o** the diastereoselectivity of the reaction was reversed and highly syn selective reactions were observed (Table 1, entries 2 and 3)! In the anti manifold, phosphoramidate **7a** was highly enantioselective, but all of the other catalysts were less selective. There is a general trend in the enantiomeric excess of the anti products and the syn/anti ratio of the reactions; i.e.,

(15) Denmark, S. E.; Su, X.; Nishigaichi, Y.; Coe, D. M.; Wong, K.-T.; Winter S. B. D.; Choi, J. Y. *J. Org. Chem.* **1999**, *64*, 1958–1967.

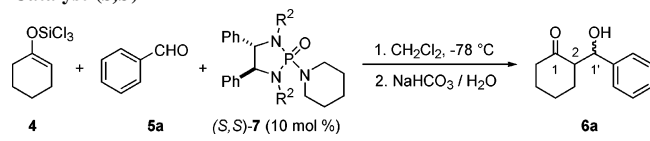
TABLE 1. Influence of External Substituents in Catalyst 7


entry	cat.	NR ^{3,2}	syn/anti ^a	syn er ^b (config)	anti er ^b (config)	yield, ^c %
1	7m^d	NMe ₂	1/19	61.5/38.5 (2 <i>S</i> ,1' <i>S</i>)	93.3/6.7 (2 <i>R</i> ,1' <i>S</i>)	91
2	7n^d	N(<i>n</i> -Pr) ₂	16/1	52.4/47.6 (2 <i>R</i> ,1' <i>R</i>)	81.1/18.9 (2 <i>R</i> ,1' <i>S</i>)	89
3	7o^d	N(<i>i</i> -Pr) ₂	32/1	50.0/50.0	60.0/40.0 (2 <i>R</i> ,1' <i>S</i>)	90
4	7p^e	NPh ₂	1/1.9	50.0/50.0	70.6/29.4 (2 <i>S</i> ,1' <i>R</i>)	86
5	7q^d	N(CH ₂) ₄	1/8.9	54.6/45.4 (2 <i>S</i> ,1' <i>S</i>)	88.0/12.0 (2 <i>R</i> ,1' <i>S</i>)	89
6	7a^d	N(CH ₂) ₅	1/60		96.0/4.0 (2 <i>R</i> ,1' <i>S</i>)	94

^a Determined by ¹H NMR analysis of the crude product mixture.^b Determined by CSP HPLC analysis; absolute configuration was assigned by the elution order from CSP HPLC. ^c Chromatographically homogeneous material. ^d (*S,S*)-Catalyst was used. ^e (*R,R*)-Catalyst was used.

higher enantioselectivity corresponds to a lower syn/anti ratio except in entry 2, which was highly syn selective but with moderate enantioselectivity of the anti product. The enantioselectivities of the syn products were low in all reactions, even in highly syn selective reactions.

2.1.1.2. Survey of Internal Substituents. The effects of the internal substituents on the nitrogens of the 2,5-diazaphospholidine ring were next to be examined. While maintaining the external piperidiny unit, stilbene-1,2-diamine derivatives bearing modifications at the *N,N'* positions were employed to provide a series of phosphoramides containing variations around the 2,5-diazaphospholidine skeleton. The results are collected in Table 2.

TABLE 2. Influence of the Internal Nitrogen Substituents in Catalyst (*S,S*)-7


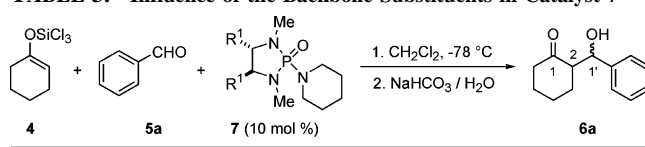
entry	cat.	R ²	syn/anti ^a	syn er ^b (config)	anti er ^b (config)	yield, ^c %
1	7h	H	> 50/1	54.6/45.4 (2 <i>R</i> ,1' <i>R</i>)		26
2	7a	Me	1/60		96.0/4.0 (2 <i>R</i> ,1' <i>S</i>)	94
3	7i	Et	1/2.0	52.4/47.6 (2 <i>R</i> ,1' <i>R</i>)	94.4/5.6 (2 <i>R</i> ,1' <i>S</i>)	92
4	7j	Ph	97/1	76.7/23.3 (2 <i>R</i> ,1' <i>R</i>)		94
5	7k	1-naphthyl	44/1	64.3/35.7 (2 <i>R</i> ,1' <i>R</i>)		31
6 ^d	7k	1-naphthyl	45/1	73.0/27.0 (2 <i>R</i> ,1' <i>R</i>)		52

^a Determined by ¹H NMR analysis of the crude product mixture.^b Determined by CSP HPLC analysis; absolute configuration was assigned by the elution order from CSP HPLC. ^c Chromatographically homogeneous material. ^d 100 mol % of **7k** was used.

With the exception of **7h** (R² = H), which afforded poor yields and little to no enantioselectivity, increasing the size of the *N,N'* substituents on the 2,5-diazaphospholidine ring in-

creased the formation of syn product. Additionally, as exemplified by the use of **7k**, extremely bulky substituents proximal to the Lewis-basic oxygen diminish the relative rates of aldol additions. Again, the parent phosphoramide **7a** was the best catalyst in terms of enantioselectivity (Table 2, entry 2). Ethyl substituents at the R² position in **7** resulted in only a slight decrease in enantioselectivity of the anti product (with the same sense of asymmetric induction), but dramatically decreased diastereoselectivity (Table 2, entry 3). Aromatic groups on this position constituted highly syn-selective catalysts (Table 2, entries 4 and 5), although only moderate enantioselectivity was observed in the syn manifold. Phosphoramide **7k** appeared highly congested, and indeed its ¹H NMR, ¹³C NMR, and ³¹P NMR clearly showed the coexistence of several rotamers at room temperature. This also explains the slow reaction in the system and low yield. Even with 1 equiv of **7k**, the reaction only gave 52% yield of the syn product with 46% ee (Table 4, entry 6). Hydrogen substitutions at the internal position (**7h**) resulted in many side reactions including deprotonation of the phosphoramide, and a very low yield of the syn product was obtained with poor enantioselectivity (Table 2, entry 1).

2.1.1.3. Survey of the Backbone Substituents. Having surveyed the effects of modifications to the external nitrogen, in addition to the ring substituents proximal to the Lewis-basic oxygen, we next turned our attention to studying the effects on rate and selectivity by modification of the chiral backbone. Table 3 compiles the results with different phosphoramides.

TABLE 3. Influence of the Backbone Substituents in Catalyst 7


entry	cat.	R ¹	syn/anti ^a	syn er ^b (config)	anti er ^b (config)	yield, ^c %
1	7a^d	Ph	1/46	58.3/41.7 (2 <i>S</i> ,1' <i>S</i>)	95.5/4.5 (2 <i>R</i> ,1' <i>S</i>)	88
2	7b^e	4-CF ₃ C ₆ H ₄	1/2.5	60.0/40.0 (2 <i>R</i> ,1' <i>R</i>)	92.3/7.7 (2 <i>S</i> ,1' <i>R</i>)	80
3	7c^e	4-MeOC ₆ H ₄	1/53	65.5/34.5 (2 <i>R</i> ,1' <i>R</i>)	96.0/4.0 (2 <i>S</i> ,1' <i>R</i>)	80
4	7d^d	3,5-Me ₂ C ₆ H ₃	1/10	69.7/30.3 (2 <i>S</i> ,1' <i>S</i>)	90.5/9.5 (2 <i>R</i> ,1' <i>S</i>)	98
5	7e^d	cyclohexyl	69/1	52.4/47.6 (2 <i>R</i> ,1' <i>R</i>)		71
6	7f^f	1-naphthyl	1/3.0			82
7	7g^e	2-naphthyl	1/56		96.0/4.0 (2 <i>S</i> ,1' <i>R</i>)	76

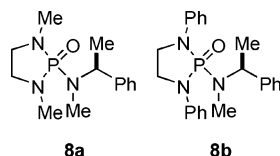
^a Determined by ¹H NMR analysis of the crude product mixture.^b Determined by CSP HPLC analysis; absolute configuration was assigned by the elution order from CSP HPLC. ^c Chromatographically homogeneous material. ^d (*S,S*)-Catalyst was used. ^e (*R,R*)-Catalyst was used. ^f Racemic catalyst was used.

All the phosphoramides used in this study were efficient catalysts and gave good to high yields of products. Aromatic substituents on the R¹ position all provided anti-selective reactions, while the cyclohexyl group gave a highly syn-selective reaction with essentially no enantioselectivity (Table 3, entry 5). Catalysts bearing electron-withdrawing groups such as in **7b** appear to be less anti selective than their counterparts containing electron-donating groups **7c** (Table 3, entries 2 and 3). Phosphoramides with sterically demanding groups such as 3,5-dimethylphenyl and 1-naphthyl were also less anti selective (Table 3, entries 4 and 6). The enantioselectivity of the anti

products was high in all cases with the same sense of asymmetric induction. Slightly lower enantioselectivities were observed for **7b** and **7d** (92.3/7.7 and 90.5/9.5 er, respectively). Parallel experiments showed that both **7c** and **7g** gave nearly identical results as the parent phosphoramidate **7a** in terms of both diastereoselectivity and enantioselectivity (Table 3, entries 3 and 7 vs entry 1). The enantioselectivity in the syn manifold was low, but the same sense of asymmetric induction was observed for entries 1–4 in Table 5. Phosphoramidate **7f** was highly congested as judged by rotamers observed by NMR spectroscopy at room temperature and 60 °C. Because of the low selectivity obtained with **7f**, resolution of the precursor diamine was not attempted.

2.1.1.4. Phenethylamine-Derived Phosphoramidates. Chiral phosphoramidates **8** derived from (*S*)-1-phenethylamine were also synthesized and used in the asymmetric aldol reaction, Chart 2. Both catalysts afforded aldol products **6a** in greater than 97% yields. With methyl groups on the internal nitrogens, **8a** was slightly anti selective while **8b**, with sterically more demanding phenyl groups in the internal positions, was highly syn selective, providing 1/4.2 and 59/1 syn/anti, respectively. Enantioselectivities for both reactions were low, less than 58.3/41.7 er, and a switch of absolute configuration of the anti product was observed from **8a** to **8b**.

CHART 2



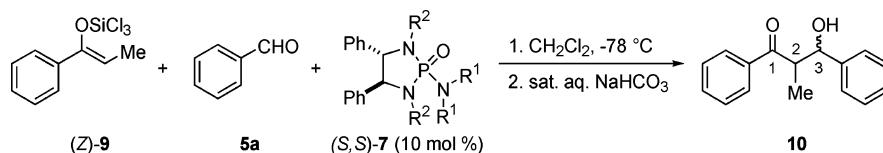
2.1.2. Reaction with Propiophenone-Derived Enolate 9. To evaluate the effects of different catalysts on the aldol addition of enolates bearing the opposite geometric configuration, several phosphoramidates were examined in the reaction of (*Z*)-**9**¹² and **5a**, Table 4.

All the phosphoramidates, with the exception of **7q**, gave good yields of the aldol products with the parent phosphoramidate **7a** still affording the best selectivities. In general, the diastereoselectivity for enolate (*Z*)-**9** was less than that of enolate **4**. As

observed previously, increasing the steric bulk around the Lewis-basic oxygen produces a shift in diastereoselectivity. While both **7a** and **7m** gave syn products, the sterically more demanding catalysts **7n** and **7i** gave anti products preferentially (Table 4, entries 3 and 4). The enantioselectivities of the syn products were high for **7a** (97.0/3.0 er) and **7m** (90.9/9.1 er) and only moderate for the relatively bulky, anti-selective catalysts **7n** and **7i**. In fact, the enantioselectivities for the anti products were low for all the catalysts (from 54.6/45.4 to 65.5/34.5 er). In the syn manifold the major enantiomer had the absolute configuration (2*S*,3*S*) except **7n**, which gave the syn product with (2*R*,3*R*) configuration. All the anti products had the (2*R*,3*S*) configuration although the enantioselectivities were low.

2.2. Survey of Achiral Phosphoramidates. In view of the dramatic effects of substituents demonstrated for the chiral catalysts, a series of structurally simpler achiral phosphoramidates was prepared. Because the level of diastereo- and enantioselectivities were generally not coupled within the phosphoramidate-catalyzed aldol additions, a diverse series of achiral agents should allow for a better understanding of the factors governing the mode of diastereoselection.

2.2.1. Reaction with Cyclohexanone-Derived Enolate 4. HMPA and two series of achiral phosphoramidates **11** and **12** having the basic diazaphospholidine skeleton were used in the reaction of enolate **4** and benzaldehyde, Table 5. By analogy to the studies involving chiral phosphoramidates, increasing steric bulk around the site of coordination decreases the relative rate of reaction and alters the diastereoselectivity from anti to syn. Thus, phosphoramidates **11a**, **11c**, **11d**, and **12a** were faster acting catalysts than the acyclic phosphoramidate HMPA, whereas **11b** was comparable to HMPA (Table 5, entry 3) and **12b** was significantly slower than HMPA (Table 5, entry 7). It is interesting to note that phosphoramidate **11d**, which is more sterically hindered than **11b**, actually gave a higher conversion than **11b** after 8 min at –78 °C (Table 5, entry 5 vs entry 3). Only **11a** and **12a** gave moderately anti selective reactions (Table 5, entries 2 and 6) while the remainder of the catalysts were syn selective (syn/anti ranging from 3.3/1 to 38/1). The synthetic utility of these catalysts was also demonstrated in preparative experiments that were allowed to proceed to

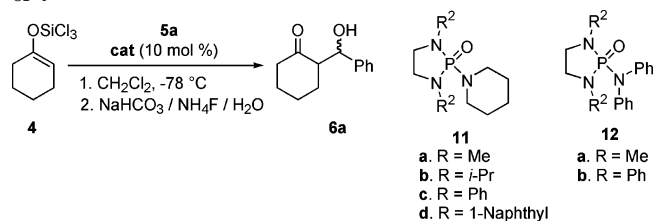
TABLE 4. Influence of Phosphoramidate Structure on the Selectivities of Reaction with (*Z*)-**9**

entry	cat.	R ¹ /R ²	syn/anti ^a	syn er ^b (config)	anti er ^c (config)	yield, ^d %
1	7a	(CH ₂) ₅ /Me	12/1	97.0/3.0 (2 <i>S</i> ,3 <i>S</i>)	54.6/45.4 (2 <i>R</i> ,3 <i>S</i>)	77
2	7m	Me/Me	5.7/1	90.9/9.1 (2 <i>S</i> ,3 <i>S</i>)	60.0/40.0 (2 <i>R</i> ,3 <i>S</i>)	74
3	7n	<i>i</i> -Pr/Me	1/9.0	70.6/29.4 (2 <i>R</i> ,3 <i>R</i>)	63.0/37.0 (2 <i>R</i> ,3 <i>S</i>)	77
4	7q	(CH ₂) ₄ /Me	1/1.6	50.0/50.0	65.5/34.5 (2 <i>R</i> ,3 <i>S</i>)	41
5	7i	(CH ₂) ₅ /Et	1/1.3	72.2/27.8 (2 <i>S</i> ,3 <i>S</i>)	56.5/43.5 (2 <i>R</i> ,3 <i>S</i>)	74

^a Determined by ¹H NMR analysis of the crude product mixture. ^b Determined by CSP HPLC analysis; absolute configuration was assigned by the elution order from CSP HPLC. ^c Absolute configuration was tentatively assigned by comparison to the literature value of optical rotation.^{16,17} ^d Chromatographically homogeneous material.

completion. All of the catalysts gave high yield of the aldol products after 1.5 to 6 h at -78°C with essentially the same selectivities (see the last two columns in Table 5).

TABLE 5. Achiral Phosphoramides in Catalyzed Aldol Additions of **4**

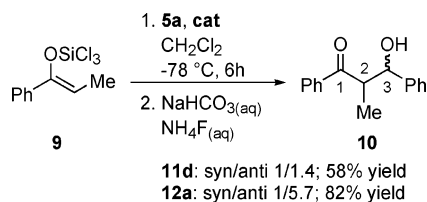


entry	cat.	conversion, ^a %	syn/anti ^b	time, h	syn/anti ^b	yield, ^c %
1	HMPA	38	3.3/1			
2	11a	82	1/2.6	1.5	1/2.8	99
3	11b	35	38/1	6.0	27/1	93
4	11c	76	16/1	1.5	31/1	96
5	11d	83	19/1	1.5	40/1	95
6	12a	87	1/1.6	3.0	1/2.7	96
7	12b	8	20/1			

^a Determined as the ratio of remaining benzaldehyde and products by ^1H NMR analysis of the crude product mixture after 8 min. ^b Determined by ^1H NMR analysis of the crude product mixture. ^c Chromatographically homogeneous material.

2.2.2. Reaction with Propiophenone-Derived Enolate **9.** As with the chiral phosphoramides, the effect of the achiral catalysts on the reaction of *Z*-enolates was evaluated. Thus, phosphoramides **11d** and **12a** were also used in the reaction of (*Z*)-**9** with benzaldehyde. With 15 mol % of **11d** or **12a**, the aldol products **10** were obtained in 58% or 82% yields with moderate anti selectivity, Scheme 4.

SCHEME 4



2.3. Influence of Substrate/Catalyst Stoichiometry. **2.3.1. Chiral Phosphoramides.** In the process of optimizing the conditions for the asymmetric aldol addition of **4** to benzaldehyde, an interesting catalyst loading effect was discovered. Initial studies with an acetone derived enolate (vide infra) suggested that reactions at low catalyst loadings and 0.1 M were slow, so the present phosphoramidate loading study with enolate **4** was performed at 0.5 M concentration, Table 6. Interestingly, as the catalyst loading was reduced the process became less anti selective. In addition, simply changing the concentration of the reaction also significantly lowered the diastereomeric ratio of the product (compare entries 1 and 4 in Table 6). Even more interesting was the fact that the enantiomeric ratio of the anti-isomer remained essentially unchanged throughout the range of catalyst loadings examined. This suggests that the diastereo- and enantioselectivity determining factors are independent and

that the syn and anti pathways are mechanistically distinct. In other words, although the syn and anti pathways are governed by the concentration of catalyst, the enantioselectivity of the individual pathways remains constant regardless of catalyst concentration. This possibility had been previously encountered in our work with cyclopentanone and cycloheptanone derived enolates wherein the rate of addition of benzaldehyde was critical to obtain high diastereoselectivity.^{5c} When the aldehyde was added slowly, high and reproducible anti-selectivity was obtained; with fast addition, lower and variable diastereoselectivity was observed. In this case as well, the enantiomeric ratio of the anti-configured products was essentially constant over a range of reaction conditions, suggesting the presence of two mechanistically distinct pathways.

TABLE 6. Phosphoramidate Loading Effects in Aldol Addition with **7a**

entry	loading, mol %	conc, M	syn/anti ^a	er (syn) ^b	er (anti) ^{b,c}	yield, ^d %
1	10	0.5	1/14	60.0/40.0	94.4/5.6	94
2	5	0.5	1/10	56.5/43.5	94.7/5.3	90
3	2	0.5	1/2.4	56.5/43.5	93.8/6.2	84
4	10	0.1	1/28	60.0/40.0	95.5/4.5	90
5	100	0.1	1/95	77.8/22.2	95.7/4.3	97

^a Determined by ^1H NMR analysis. ^b Determined by CSP HPLC analysis. ^c (2*R*,1'*S*)/(2*S*,1'*R*). ^d Chromatographically homogeneous material.

Under the hypothesis that the “slow addition effect” should be relevant in the reaction with enolate **4** as well, another catalyst loading study with **7a** was conducted, this time with the aldehyde added slowly over roughly 1 h, Table 7. Clearly there is a dramatic effect, as the level of diastereoselectivity changed from 1/2.4 to 1/28 with 2 mol % catalyst for fast and slow additions of benzaldehyde, respectively. In fact, even with 0.5 mol % catalyst, the reaction is moderately anti selective (syn/anti = 1/5). As before, the enantioselectivity of the anti process remained unchanged, even over a 20-fold change in phosphoramidate loading.

TABLE 7. Catalyst Loading Effect with **7a** and Slow Addition of Benzaldehyde

entry	loading, mol %	syn/anti ^b	er (syn) ^c	er (anti) ^{c,d}	yield, ^e %
1	10	<1/50	58.3/41.7	95.5/4.5	94
2	2	1/28	52.4/47.6	95.7/4.3	96
3	0.5	1/5	52.4/47.6	95.5/4.5	53

^a 1 h addition time to a final concentration of 0.1 M. ^b Determined by ^1H NMR analysis. ^c Determined by CSP SFC analysis. ^d (2*R*,1'*S*)/(2*S*,1'*R*). ^e Chromatographically homogeneous material.

In a more complete catalyst loading study involving the acetone-derived trichlorosilyl enolate **1**, a less dramatic effect was observed, Table 8. Above a ceiling catalyst loading (roughly 5 mol %) there was little variation in the enantiomeric ratio of

(16) Ishihara, K.; Maruyama, T.; Mouri, M.; Gao, Q.; Furuta, K.; Yamamoto, H. *Bull. Chem. Soc. Jpn.* **1993**, 66, 3483–3491.

(17) Juaristi, E.; Beck, A. K.; Hansen, J.; Matt, T.; Mukhopadhyay, T.; Simson, M.; Seebach, D. *Synthesis* **1993**, 1271–1290.

the aldol adduct even up to 20 mol % of phosphoramidate. However, when even lower phosphoramidate loadings (down to 1 mol %) were used, the enantiomeric ratio of the product dropped slightly, though the yield of the overall process remained high when the reaction was performed at 0.5 M. This effect stands in contrast to the lack of an enantioselectivity dependence on catalyst loading in the aldol additions with the cyclohexanone-derived enolate **4** above; perhaps suggesting the origin of the diminished enantioselectivity at lower catalyst loading in **1** is connected to the factors controlling diastereoselectivity for reactions of **4** (vide infra).¹⁸

TABLE 8. Catalyst Loading Effect with **7a**^a

$\text{Me}-\text{C}(\text{OSiCl}_3)=\text{CH}_2 \xrightarrow[2. \text{NaHCO}_3(\text{sat, aq})]{1. \text{5a, (S,S)-7a, CH}_2\text{Cl}_2, -78^\circ\text{C}} \text{Me}-\text{C}(=\text{O})-\text{CH}(\text{OH})-\text{Ph}$				
13		14		
entry	loading, mol %	conc, M	er ^b (S/R)	yield, % ^c
1	20	0.1	92.3/7.7	82
2	10	0.1	91.7/8.3	90
3	10 ^d	0.5	7.7/92.3	87
4	5	0.5	92.3/7.7	88
5	3	0.5	89.6/10.4	86
6	2	0.5	88.6/11.4	88
7	1	0.5	83.6/16.4	92

^a 1 h addition time to a final concentration of 0.1 M. ^b Determined by CSP HPLC analysis of the corresponding 2,4-dinitrophenyl carbamates. ^c Chromatographically homogeneous material. ^d Performed with 10 mol % of (R,R)-**7a**.

2.3.2. Achiral Phosphoramidates. 2.3.2.1. Reaction with Cyclohexanone-Derived Enolate 4. The dependence of the diastereomeric ratio of the aldol products on the catalyst loading has also been observed with the achiral catalysts. In the reaction of **4** and **5a**, the ratio of phosphoramidate **11c** to the enolate **4** was very important in determining the syn/anti ratio of product **6a**. Under otherwise identical conditions, the syn/anti ratio of **6a** was 130/1 when 2 mol % of **11c** was used, and the ratio dropped to 2/1 when 200 mol % of the same catalyst was used, Table 9. A detailed study on this intriguing loading effect was undertaken, and the results are depicted in Figure 2.

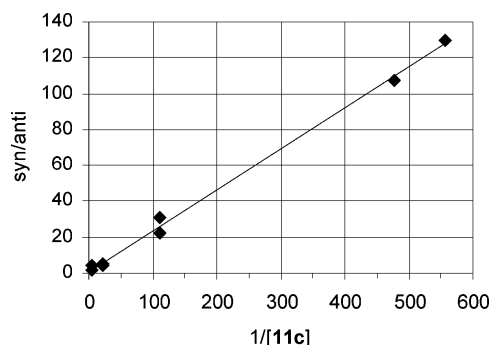


FIGURE 2. Dependence of product syn/anti ratio on the loading of **11c**.

(18) It should be noted that methyl ketone derived trichlorosilyl enolates are less reactive than the cyclohexanone derived enolate **4**. In a control experiment, the trichlorosilyl enolate derived from methyl *n*-butyl ketone and 4-phenylbenzaldehyde were stirred at -78°C for 2 h, providing only 4% of the corresponding aldol adduct, with 95% recovery of the unchanged aldehyde after column chromatography.

TABLE 9. Loading Effect for the Addition of **4** to Benzaldehyde Using Catalyst **11c**^a

$\text{Cyclohexanone-OSiCl}_3 \xrightarrow[2. \text{NaHCO}_3 / \text{NH}_4\text{F} / \text{H}_2\text{O}]{1. \text{5a (2.0 equiv), 11c, CH}_2\text{Cl}_2, -78^\circ\text{C}, 1.5-6\text{h}} \text{Aldol product 6a}$			
entry	loading, mol %	dr, ^b syn/anti	yield, ^c %
1	1.8	130/1	95
2	2.1	107/1	97
3	9.1	31/1	96
4	9.1	22/1	97
5	46	4.8/1	83
6	46	4.4/1	95
7	194	1.4/1	97
8	201	1.3/1	96

^a 1 h addition time to a final concentration of 0.1 M. ^b Determined by ¹H NMR analysis. ^c Chromatographically homogeneous material.

At lower catalyst loading, higher syn/anti ratio was observed. A straight line with good correlation ($R^2 = 0.997$) was obtained when the syn/anti ratio was plotted against $1/[\mathbf{11c}]$. This dramatic influence of the catalyst loading on selectivity clearly implies the simultaneous operation of competitive pathways in the reaction (vide infra).

Phosphoramidate **12a** also showed a loading dependence in the reaction of **4** and **5a** (Table 10), albeit a much smaller effect was observed, Figure 3. The catalyst **12a** was moderately anti selective (syn/anti 1/7–8) at high catalyst loadings while slightly syn selective (syn/anti 1.2/1) at lower catalyst loadings (2.1 mol %). Again a linear relationship can be derived between the syn/anti ratio and $1/[\mathbf{12a}]$ ($R^2 = 0.988$).

TABLE 10. Loading Effect for the Addition of **4** to Benzaldehyde Using Catalyst **12a**^a

$\text{Cyclohexanone-OSiCl}_3 \xrightarrow[2. \text{NaHCO}_3 / \text{NH}_4\text{F} / \text{H}_2\text{O}]{1. \text{5a (2.0 equiv), 12a, CH}_2\text{Cl}_2, -78^\circ\text{C}, 1.5-6\text{h}} \text{Aldol product 6a}$			
entry	loading, mol %	dr, ^b syn/anti	yield, ^c %
1	2.1	1.2/1	96
2	2.4	1.0/1	92
3	5.4	1/1.6	98
4	9.4	1/2.7	96
5	9.5	1/2.4	97
6	19.7	1/4.3	99
7	46	1/7.9	90
8	49	1/8.1	93
9	195	1/6.8	91
10	199	1/6.1	ND

^a 1 h addition time to a final concentration of 0.1 M. ^b Determined by ¹H NMR analysis. ^c Chromatographically homogeneous material.

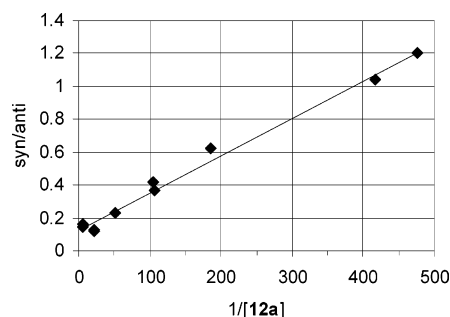
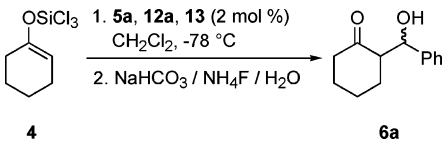


FIGURE 3. Loading effects of **12a** in the reaction of **4** with benzaldehyde.

2.3.2.2. Propiophenone-Derived Enolate 9. Whereas the reaction with enolate **4** showed dramatic dependence of product syn/anti ratio on catalyst loading, the reaction with enolate **9** was essentially independent of catalyst loading. With catalyst **11d**, in a 7-fold range of the catalyst loadings, 14–98 mol %, the reaction produced essentially the same syn/anti ratio, 1/1.4 to 1/1.5. With catalyst **12a** the syn/anti ratio increased slightly (1/5.7 to 1/4.1) in a 6.7-fold increase of catalyst loadings from 15 to 100 mol %.

2.3.3. The Effects of Acids on the Aldol Addition Reactions. In the course of these loading effect studies we noticed that a small amount of benzoic acid (**13**), which was present as a contaminant in the benzaldehyde used, dramatically altered the syn/anti ratio of the reaction with enolate **4**. Freshly distilled benzaldehyde was stored under nitrogen in the freezer, but after several days a small amount of benzoic acid may accumulate and can be subsequently detected by ^1H NMR. Table 11 lists the results of a loading study with **12a** and obtained with benzaldehyde spiked with 2% of benzoic acid.

TABLE 11. Benzoic Acid Effects on Syn/Anti Ratio of the Aldol Addition Reactions

			
entry	loading 12a , mol %	syn/anti ^a	yield, ^b %
1	2.0	72/1	81
2	3.6	33/1	95
3	5.6	23/1	85
4	7.3	4.0/1	90
5	9.1	1/1.1	98
6	18.4	1/2.9	95

^a Determined by ^1H NMR analysis of the crude product mixture.
^b Chromatographically homogeneous material.

With catalyst **12a**, which was unselective in the reaction of enolate **4** with benzaldehyde (see Table 5, entry 6), the reaction became highly syn selective at low loadings in the presence of benzoic acid (Table 11, entry 1). The yields of all the reactions were high. A comparison of the loading effects with and without benzoic acid is plotted in Figure 4. This dramatic increase in the stereoselectivity only manifests itself at lower catalyst loading. At higher catalyst loading the impact of small amount

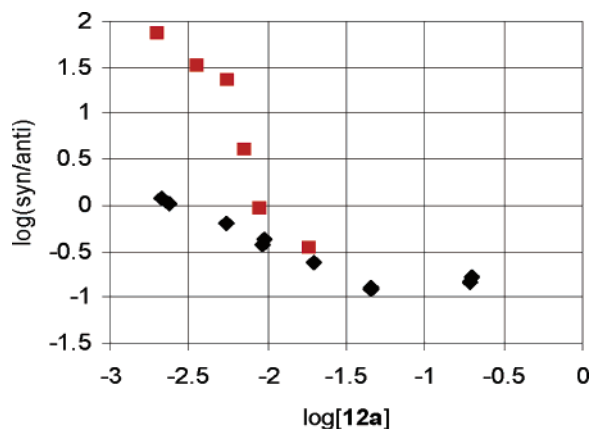
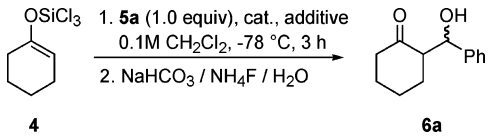


FIGURE 4. Loading effects of phosphoramidate **12a** in the presence and absence of benzoic acid (◆ without benzoic acid, ■ with benzoic acid).

of benzoic acid was minimal. To understand the nature of these effects, we initiated studies to investigate the influence of benzoic acid and other acids in the reaction.

In the reaction of enolate **4** and freshly distilled benzaldehyde, known quantities of acids were added, and the results are listed in Table 12. Without benzoic acid, the reaction of **4** and **5a** was catalyzed by 2 mol % of phosphoramidate **12a** to give high yield of the aldol products **6a** in a syn/anti ratio of 1.2/1 (Table 12, entry 1). In the presence of 2 mol % benzoic acid the reaction yield was still good and the syn/anti ratio increased to 89/1 (Table 12, entry 2). With (*S*)-mandelic acid (10 mol %) and **12a** (9.6 mol %), the reaction was again highly syn selective and afforded a high yield of product, but with no detectable enantiomeric enrichment (Table 12, entry 3). Strong acids such as triflic acid inhibited the catalytic ability of **12a**, and the results observed were essentially the same as the background reaction (Table 12, entry 4). With phosphoramidate **11c** a similar increase in the syn selectivity by benzoic acid was observed (Table 12, entries 5 and 7 vs entries 6 and 8) although the effects were much less dramatic as in the case of **12a**. In the absence of phosphoramidate, benzoic acid itself (2 mol %) did not promote the reaction and only a background reaction was observed (Table 12, entry 9).

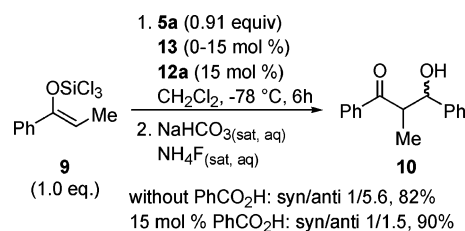
TABLE 12. Acid Effects in the Reaction between **4** and Benzaldehyde^a

				
entry	cat. ^a (mol %)	additive ^a (mol %)	syn/anti ^b	yield, ^c %
1	12a (2.1)	none	1.2/1	96
2	12a (2.0)	PhCO ₂ H (2.0)	89/1	87
3	12a (9.6)	(<i>S</i>)-mandelic acid (10)	76/1	84 ^d
4	12a (2.1)	CF ₃ SO ₃ H (2.1)	140/1	25
5	11c (2.1)	none	107/1	97
6	11c (2.0)	PhCO ₂ H (2.0)	200/1	97
7	11c (9.1)	none	22/1	97
8	11c (9.8)	PhCO ₂ H (9.8)	45/1	92
9	none	PhCO ₂ H (2.0)	> 200/1	25

^a Relative to [**4**]. ^b Determined by ^1H NMR analysis of the crude mixture.
^c Chromatographically homogeneous material. ^d Racemic.

The reaction of enolate (*Z*)-**9** also showed a moderate benzoic acid effect, Scheme 5. In the absence of benzoic acid, the reaction of the (*Z*)-**9** with benzaldehyde gave an 82% yield of the aldol product with a syn/anti ratio of 1/5.6, while the addition of 15 mol % benzoic acid increased the syn/anti ratio to 1/1.5. Thus, with both *Z*- and *E*-enolates, the effect of benzoic acid was to increase the syn selectivity of the reactions.

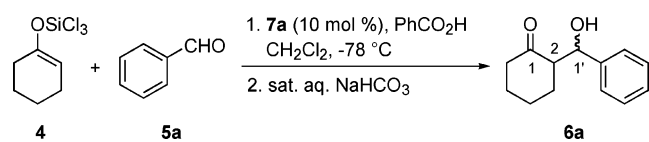
SCHEME 5



Pronounced benzoic acid effects have also been found in the aldol addition reaction of **4** and **5a** catalyzed by **7a**, Table 13.

With freshly distilled benzaldehyde, the reaction was highly anti selective and highly enantioselective in the anti manifold (Table 13, entry 1). With 1 mol % of benzoic acid, only a slight decrease in anti selectivity and yield was observed (Table 13, entry 2 vs entry 1). With 10 mol % benzoic acid (equivalent to phosphoramidate **7a**), the reaction becomes syn selective and much slower than the reaction without benzoic acid (only 24% conversion after 8 min, Table 13, entry 3). The syn product from the reaction with 10 mol % of benzoic acid was essentially racemic while the anti product had decreased enantioselectivity compared to entry 1. The reaction with 20 mol % of benzoic acid was also rather slow. After extended time (2 h) the reaction was highly syn selective although the conversion was still low (62%, Table 13, entry 4). The syn product from the reaction was racemic, while the anti product showed moderate enantioselectivity (77.3/22.7 er).

TABLE 13. Benzoic Acid Effect in the Reaction Promoted by Chiral Catalyst **7a**

							
entry	PhCO ₂ H, mol %	time, min	syn/anti ^b	conv, % ^c	syn er ^d (config)	anti er ^d (config)	yield, ^e %
1 ^a	0	8	1/28	100	54.6/45.4 (2 <i>S</i>)	95.5/4.5 (2 <i>R</i>)	96
2	1	8	1/17	91	54.6/45.4 (2 <i>S</i>)	95.5/4.5 (2 <i>R</i>)	90
3	10	8	4.1/1	24	50.0/50.0	89.0/11.0 (2 <i>R</i>)	18
4	20	120	18/1	62	50.0/50.0	77.3/22.7 (2 <i>R</i>)	60

^a Parallel with other experiments in the table. ^b Determined by ¹H NMR analysis of the crude product mixture. ^c Determined as the ratio of remaining benzaldehyde and products by ¹H NMR analysis of the crude product mixture. ^d Determined by CSP HPLC analysis; absolute configuration was assigned by the elution order from CSP HPLC. ^e Chromatographically homogeneous material.

2.4. Nonlinear Effects. From the loading effect studies, we hypothesized that catalyst concentration dependent stereoselectivity is indicative of competing reaction pathways involving different molecularity in the transition structure assembly. We reasoned that if more than one phosphoramidate were indeed involved in one of the pathways (syn- or anti-selective) then nonlinear effects¹⁹ could be observed with nonracemic phosphoramidate **7a**. Moreover, if one of the two pathways proceeds through a transition structure involving only one phosphoramidate bound to silicon, then a linear relationship should exist between the enantiomeric composition of the aldol product and the catalyst enantiopurity.

2.4.1. The Anti Manifold. Enantioenriched samples of the phosphoramidate were prepared by weighing the calculated amounts of (*S,S*)-**7a** and (*R,R*)-**7a** into the reaction vessel which was then dried under high vacuum. The phosphoramidates were then dissolved in methylene chloride under argon and used in aldol additions of **4** to **5a** at -78°C . The results for 20, 40, 60, and 80% ee catalyst showed a positive nonlinear effect when

employing 10 mol % of phosphoramidate **7a**, Figure 5. Thus, with 40% ee of catalyst **7a**, the anti product **6a** was obtained in 53% ee (76.7/23.3 er).²⁰

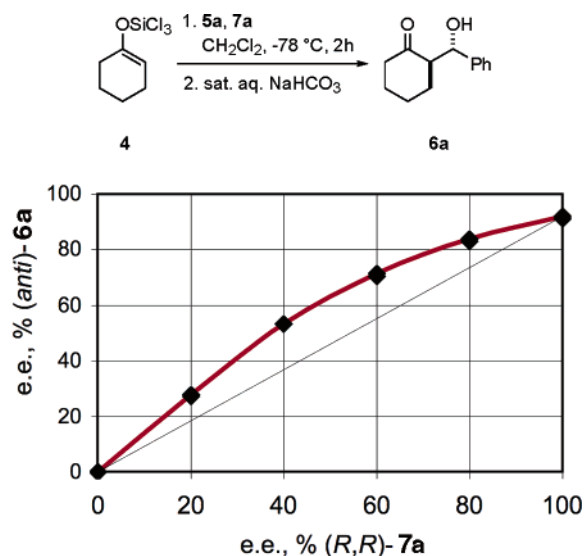


FIGURE 5. Relationship between the enantiopurity of *anti*-**6a** and (*R,R*)-**7a**.

The above data fits very well with Kagan's two-ligand model.²¹ Thus, assuming two chiral ligands are involved in the stereodetermining transition structure and assuming a statistical distribution of the enantiomeric ligands, the enantioselectivity of the product (ee_{prod}) and the enantiopurity of the ligands (ee_{cat}) are related by the following equation

$$ee_{\text{prod}} = ee_0 ee_{\text{cat}} \frac{2}{1 + g + (1 - g)ee_{\text{cat}2}} \quad (1)$$

where ee_0 is the product enantioselectivity when ee_{cat} equals 100% and $g = k_{\text{RS}}/k_{\text{RR}}$, where $k_{\text{RS}}/k_{\text{RR}}$ is the ratio of the rate constants through heterodimeric (k_{RS}) and homodimeric (k_{RR}) transition states. An iterative line fitting of the data in Figure 5 to the above equation gave $g = 0.277$ with $R^2 = 1.000$. Therefore, the calculated reaction rate constant of a heterodimeric transition structure is about 28% of that of a homodimeric transition structure.

2.4.2. The Syn Manifold. Enantioenriched phosphoramidate **7j** was prepared in a similar manner as above. Thus, the calculated amounts of the corresponding (*S,S*)-**7j** and (\pm)-**7j** were weighed into a reaction vessel which was then dried under high vacuum. The phosphoramidates were then dissolved in methylene chloride under argon and employed in aldol additions.

The results for 0, 20, 40, 60, 80, and 100% ee of catalyst **7j** were plotted in Figure 6, and indeed, a linear relationship between the syn product enantioselectivity and the enantiopurity

(20) For discussion of nonlinear effects, the use of enantiomeric excess (ee) is preferred. For an discussion of the relative merits of er vs ee, see: (a) Kagan, H. B. *Recl. Trav. Chem. Pays-Bas* **1995**, *114*, 203–205. (b) Schurig, V. *Enantiomer* **1996**, *1*, 139–143. Gawley, R. E. *J. Org. Chem.* **2006**, *73*, 2411–2416.

(21) (a) Fenwick, D. R.; Kagan, H. B. *Top. Stereochem.* **1999**, *22*, 257–296. (b) Girard, C.; Kagan, H. B. *Angew. Chem., Int. Ed.* **1998**, *22*, 2922–2959. (c) Avalos, M.; Babiano, R.; Cintas, P.; Jiménez, J. L.; Palacios, J. C. *Tetrahedron: Asymmetry* **1997**, *8*, 2997–3017.

(19) (a) Puchot, C.; Samuel, O.; Duñach, E.; Zhao, S.; Agami, C.; Kagan, H. B. *J. Am. Chem. Soc.* **1986**, *108*, 2353–2357. (b) Guillaneux, D.; Zhao, S.-H.; Samuel, O.; Rainford, D.; Kagan, H. B. *J. Am. Chem. Soc.* **1994**, *116*, 9430–9439.

of catalyst **7j** was observed with $R^2 = 0.999$. These observations strongly support the hypothesis that two phosphoramidate molecules are involved in the transition structure in the anti-selective pathway, whereas only one phosphoramidate molecule is present in the transition structure leading to the syn product.

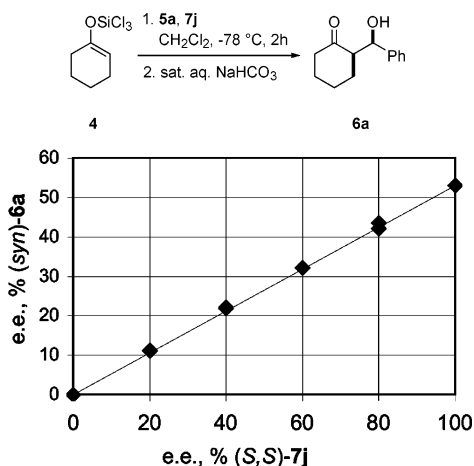


FIGURE 6. Relationship between the enantiopurity of *syn*-**6a** and *(S,S)*-**7j**.

2.4.3. Control Experiments. 2.4.3.1. Fast Quenching Experiments. An alternative rationale for the nonlinear effect is the potential interaction between the catalyst and the product. Although this “product-inhibition” process can lead to nonlinear effects, it also affects a change in enantioselectivity as a function of time. To rule out the possibility that the product from the reaction may be involved in the stereochemical determining step²² or in the nonlinear effect observed in Figure 5, the enantiomeric composition of the product as a function of conversion was determined, Table 14. With catalyst **7a** in 40% ee the conversion of the reaction was 55% after 10 s and with essentially the same enantioselectivity as at 100% conversion (Table 14, entries 1 and 3). The reaction with 10 mol % of **5a** was employed to mimic the reaction at 10% conversion and gave *anti*-**6a** with similar enantioselectivity (Table 14, entry 4). In the presence of 1 equiv of phosphoramidate **7a**, the possibility that one of the enantiomers of the phosphoramidate **7a** may be selectively bound to the product to give rise to the nonlinear effects should be minimized, and again essentially the same enantioselectivity was obtained.

TABLE 14. Control Experiments Using Enantioenriched **7a**

entry	5a , equiv	7a , equiv	time, s	conv., ^a %	yield, ^b %	er ^c (<i>anti</i> - 6a)
1	1.0	0.1	480	100	95	76.7/23.3
2	1.0	0.1	30	63	61	76.9/23.1
3	1.0	0.1	10	55	52	76.6/23.4
4	0.1	0.1	480	100	96	76.6/23.4
5	1.0	1.0	480	100	99	77.0/23.0

^a Determined by ^1H NMR analysis. ^b Chromatographically homogeneous material. ^c Determined by CSP SFC analysis.

Yet another explanation for a nonlinear effect is the existence of aggregates in the resting state of the catalyst. This so-called

“reservoir effect” has been invoked by Noyori and co-workers to explain the highly positive nonlinear effect in the diethylzinc addition of benzaldehyde catalyzed by (–)-3-*exo*-(dimethylamino)isborneol (DAIB).²³ In contrast to the results obtained by Noyori and co-workers, essentially no dependence of the degree of nonlinearity on the concentration of catalyst **7a** was observed (Table 14, entry 1 vs 5). Also, a reservoir effect cannot explain the change of diastereoselectivity on the catalyst loading. Thus, taken together, these results strongly support a transition structure with more than one phosphoramidate molecule. In addition, these control experiments clearly rule out other interpretations for nonlinear effects and support the hypothesis that two phosphoramidate molecules are present in the transition structure and are responsible for the nonlinear effects observed.

2.4.3.2. Low-Temperature NMR Studies. Several attempts were made to reveal the nature of the silicon–phosphoramidate association in the solution state.²⁴ Low-temperature experiments were designed to probe the existence of multiple complexes of phosphoramidates with SiCl_4 . Unfortunately, low-temperature ^{31}P NMR studies could not reveal any distinct signals indicative of complex formation. Rather, the presence of broad peaks and the disappearance of the original phosphorus signal upon addition of SiCl_4 suggest complexation is highly dynamic, possibly involving the rapid equilibration of multiple phosphorus–silicon complexes.²⁵

2.5. Solvent Effects and Salt Effects. 2.5.1. Solvent Effects. Given that the transition structure for these catalyzed aldolizations is proposed to involve cationic, hexacoordinate silicon species, it is reasonable to expect that the nature of the reaction medium would strongly influence both the overall rate and selectivity of the transformation. To investigate this, two solvent surveys were performed, both with fast and slow additions of **5a** (Table 15). In the first series of experiments, **5a** was added quickly to a cold (-78°C) solution of phosphoramidate (*S,S*)-**7a** (10 mol %) and **4** in various solvents (entries 1, 3, 5, and 7). The benchmark reaction proceeded with high diastereoselectivity (*anti*) and with high *er* in the *anti* manifold. The use of the less polar solvents toluene and pentane provided significantly diminished *dr* and *er*, entries 5 and 7. The relatively low yield of the reaction in pentane most likely represents the limited solubility of the phosphoramidate in this solvent at low temperature. When Et_2O was used, the diastereoselectivity of the process increased (entry 3). However, the enantioselectivity of the *anti* process decreased appreciably relative to that obtained in CH_2Cl_2 .

Subsequent reactions were carried out with 2 mol % of phosphoramidate (Table 15, entries 2, 4, 6, and 8). Clearly, solvent does have an effect on both the diastereoselectivity and the enantioselectivity of the resultant aldol adducts. Additionally, the trends are the same regardless of the reaction protocol used. Diethyl ether provided higher diastereoselectivity relative to CH_2Cl_2 , though enantioselectivity was lowered. Toluene and pentane provided low levels of both relative and absolute stereochemical control. The use of propionitrile, however, provided both high diastereoselectivity and only slightly at-

(22) Shibata, T.; Morioka, H.; Hayase, T.; Choji, K.; Soai, K. *J. Am. Chem. Soc.* **1996**, *118*, 471–472.

(23) Kitamura, M.; Okada, S.; Suga, S.; Noyori, R. *J. Am. Chem. Soc.* **1989**, *111*, 4028–4036.

(24) For X-ray crystallographic studies of phosphoramidates with tin tetrachloride, see ref 11a.

(25) For a solution NMR studies of phosphoramidates with silicon tetrachloride, see: Denmark, S. E.; Beutner, G. L.; Wynn, T.; Eastgate, M. D. *J. Am. Chem. Soc.* **2005**, *127*, 3774–3789.

tenuated enantioselectivity in comparison with CH_2Cl_2 . This result is rather surprising given the relatively high Lewis basicity of this solvent. Clearly such a nitrile donor cannot compete with the phosphoramidate catalyst, even when used as the reaction solvent. At lower catalyst loadings, a difference in rate was also apparent, with the reactions in Et_2O and toluene being significantly slower (based on yield, balance is unreacted aldehyde) than experiments performed in either CH_2Cl_2 or propionitrile.

TABLE 15. Solvent Effects in Aldol Additions of **4** Catalyzed by **7a**

entry	loading, mol %	solvent (ϵ^a)	syn/anti ^b	er (syn)	er (anti)	yield, ^c %
1	10 ^d	CH_2Cl_2 (9.1)	1/35	ND	96.2/3.8 ^e	85
2	2 ^f	CH_2Cl_2 (9.1)	1/28	1/1 ^g	95.8/4.2 ^g	91
3	10 ^d	Et_2O (4.3)	1/>50	ND	89.5/10.5 ^e	82
4	2 ^f	Et_2O (4.3)	1/49	1.5/1 ^g	87.5/12.5 ^g	59
5	10 ^d	toluene (2.4)	1/6.2	1.4/1 ^e	83.3/16.7 ^e	84
6	2 ^f	toluene (2.4)	1/5.2	1.1/1 ^g	87.2/12.8 ^g	51
7	10 ^d	pentane (1.8)	1/2	1.2/1 ^e	65.5/34.5 ^e	70
8	2 ^f	$\text{CH}_3\text{CH}_2\text{CN}$ (37.5)	1/31	1.4/1 ^g	93.3/6.7 ^g	85

^a At 20 °C, taken from the *CRC Handbook of Chemistry and Physics*, 72nd ed. ^b Determined by ^1H NMR analysis. ^c Chromatographically homogeneous material. ^d PhCHO added over 1 min/0.1 M/2 h. ^e Determined by CSP HPLC analysis. ^f PhCHO added over 1 h/0.1 M. ^g Determined by CSP SFC analysis.

When a survey of reaction solvents was performed with acetone-derived enolate **1**, a similar trend was found in the enantioselectivity of the adducts, Table 16. Both yield and selectivity were lowered dramatically on switching from CH_2Cl_2 to Et_2O , THF, or toluene. Trichloroethylene (Table 16, entry 2) provided a good yield, though with lower enantioselectivity. Again, propionitrile was a very effective solvent,

TABLE 16. Survey of Solvents on the Addition of **1** to Benzaldehyde

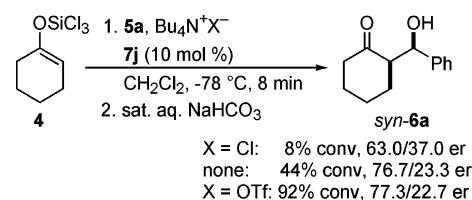
entry	solvent	er ^b	yield, ^c %
1	CH_2Cl_2	92.9/7.1	92
2	trichloroethylene	80.0/20.0	88
3	Et_2O	68.8/31.2	37
4	toluene	64.3/35.7	48
5	THF	77.3/22.7	59
6 ^d	$\text{CH}_3\text{CH}_2\text{CN}$	10.3/89.7	88

^a **5a** added over 1 min, 0.1 M/2 h. ^b Determined by CSP HPLC analysis of the corresponding 2,4-dinitrophenyl carbamates. ^c Chromatographically homogeneous material. ^d Performed with 10 mol % (*R,R*)-**7a**.

rivaling CH_2Cl_2 in both yield and enantioselectivity, though as above with **4**, the selectivity was slightly attenuated.

2.5.2. Salt Effects. All of the above studies indicated the operation of competitive pathways involving one or two phosphoramidate molecules in the transition structure for promoted aldolization of trichlorosilyl enolates. If two phosphoramidate molecules and an aldehyde coordinate to the silicon of the enolate, then ionization of a chloride ion from the trichlorosilyl enolate is required to maintain hexacoordination.²⁶ To probe the necessity of ionization, the effects of tetrabutylammonium salts on the rate and selectivities of the reaction were investigated. In the reaction promoted by phosphoramidate **7a**, tetrabutylammonium chloride or triflate gave similar results, but the reaction was too fast to conclude if these salts affect the reaction. With the slower acting catalyst **7j** (which gave 44% conversion to the syn product **6a** with 53% ee after 8 min at -78 °C), it was clearly shown that $\text{Bu}_4\text{N}^+\text{Cl}^-$ inhibits the reaction whereas $\text{Bu}_4\text{N}^+\text{OTf}^-$ accelerated the reaction, Scheme 6. Thus, in the presence of 1.2 equiv of $\text{Bu}_4\text{N}^+\text{Cl}^-$ or $\text{Bu}_4\text{N}^+\text{OTf}^-$, conversion of the reaction was 8% (63.0/37.0 er) and 92% (77.3/22.7 er), respectively. Thus, the rates of aldol addition of trichlorosilyl enolates catalyzed by phosphoramidates are greatly influenced by the presence of tetrabutylammonium salts.

SCHEME 6



2.6. Kinetics. Initial kinetic experiments were performed using catalyst **7j**. The decision to start with this phosphoramidate allowed for the study of a slower acting catalyst prior to evaluating the more active catalyst **7a**. Moreover, previous studies have suggested that **7j** proceeds through a single phosphoramidate pathway, which should provide a more tractable system for initial investigation.

2.6.1. Reactions Catalyzed by Phosphoramidate 7j. Unlike determining the kinetic order for the uncatalyzed reactions, determining order in catalyst could not be realistically accomplished using pseudo-order conditions. Rather, the rate constant for the catalyzed reaction was measured as a function of catalyst concentration. Manipulation of standard rate equations reveals that under these conditions the slope of $\log(k)$ vs $\log[\text{catalyst}]$ is equivalent to the kinetic order of the species in question, in this case the catalyst.

The order in phosphoramidate was determined by measuring the observed rate constant (k_{obs}) for the aldol reaction between cyclohexanone trichlorosilyl enolate **4** and benzaldehyde as a function of concentration near typical catalyst loadings by ReactIR analysis. Presentation of the results in a log–log plot revealed, as expected, a linear relationship with a slope nearly equal to 1, $m = 1.014$, Figure 7.

Interestingly, inspection of this function suggested that the rate did not approach zero as the concentration of catalyst approached zero. Careful extrapolation to 0 mol % catalyst gave an unrealistically high value for the theoretical background

(26) Short, J. D.; Attenoux, S.; Berrisford, D. J. *Tetrahedron Lett.* **1997**, 38, 2351–2354.

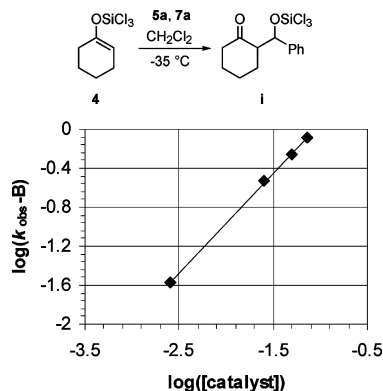


FIGURE 7. Plot of $\log(k_{\text{obs}} - B)$ versus $\log([\text{catalyst}])$ for the addition of **4** to **5a** catalyzed by **7a** at $T = -35^\circ\text{C}$. The graph depicts the linear fit to $f(x) = mx + b$ ($m = 1.014$, $R^2 = 1.000$).

reaction, as determined by earlier preparative studies. This prompted us to examine the reaction rates at much lower catalyst concentrations, Figure 8. The sharp change in slope at low catalyst loadings is consistent with a change in mechanism for this aldol addition. Indeed, these results fully support the hypothesis that the promoted pathway involves ionization of chloride and utilizes cationic silicate species whereas the unpromoted pathway does not. Inspection of Figure 8 also reveals a lower catalyst loading limit of approximately 2 mol % catalyst loading, at which the undesirable unpromoted pathway becomes competitive with the promoted pathway.

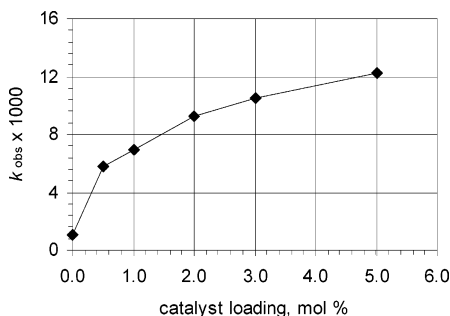


FIGURE 8. Plot of k_{obs} versus catalyst loading for the addition of **4** to **5a**, catalyzed by **7j**.

Activation parameters for the catalyzed reaction could be determined as before, now over a temperature range of -11 to -65°C , Table 17. As was observed for the uncatalyzed addition of **4** to **5a**, ΔS^\ddagger remains the predominant contributor to ΔG^\ddagger . The nearly vanishing value for ΔH^\ddagger reveals a greater level of activation for the catalyzed reaction.

TABLE 17. Arrhenius Activation Energies for the Aldol Addition of **4** to **5a** Catalyzed by **7j** as Determined by Kinetic Analysis^a

activation parameters	activation values (ReactIR)	activation values (RINMR)
ΔH^\ddagger (kcal mol ⁻¹)	0.3 ± 0.1	1.2
ΔS^\ddagger (cal mol ⁻¹ K ⁻¹)	-67.1 ± 0.7	-63.3
ΔG^\ddagger (kcal mol ⁻¹)	20.6 ± 0.2	20.4

^a Activation parameters were calculated for $T = 303\text{ K}$.

2.6.2. Reactions Catalyzed by Phosphoramidate 7a. Initial attempts to study relations catalyzed by phosphoramidate **7a** using the ReactIR techniques proved inconclusive due to extremely fast reaction rates at -65°C . Attempts to attenuate the reaction

rates by decreasing the temperature resulted in unstable baselines and inconsistent results. Furthermore, attempts to reduce the reaction rates by dilution of the reaction mixture gave poor signal-to-noise ratios. Although kinetics studies using ReactIR were inconclusive, Rapid Injection NMR (RINMR)²⁷ analysis was able to address the limitations of the previous methods. To verify the reliability of the RINMR apparatus, activation parameters for the aldol addition of **4** to **6a** catalyzed by the more bulky phosphoramidate **7j** were repeated using this instrument. Careful analysis revealed good agreement with the previous ReactIR studies, Table 17.

Thus secured, the more challenging task of studying reactions promoted using catalyst **7a** was undertaken. ¹H NMR analysis permitted operation at lower concentrations than previously possible for the reaction of **4** with **5a**. As described previously, a plot of $\log(k_{\text{obs}})$ vs $\log[\text{catalyst}]$ allowed for the determination of order in catalyst for catalyst concentrations between 0.009 and 0.016 M. When plotted, the slope of the logarithmic function (m) was determined to be 2.113, Figure 9.

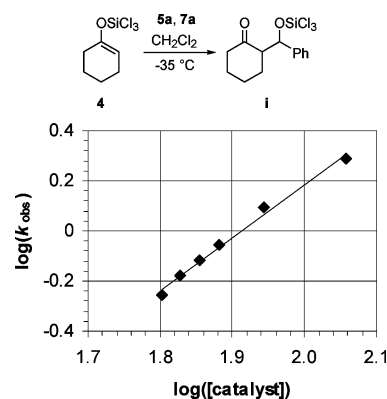


FIGURE 9. Plot of $\log(k_{\text{obs}})$ versus $\log([\text{catalyst}])$ for the addition of **4** to **6a** catalyzed by **7a** at $T = -80^\circ\text{C}$. The graph depicts the linear fit to $f(x) = mx + b$ ($m = 2.113$, $R^2 = 0.992$).

Arrhenius activation energies were then determined using 10 mol % of catalyst over a 20° temperature range, between -70 and -90°C (Table 18). Attempts to extend this range by increasing the temperature above -70°C gave reaction rates which exceeded the ability of the RINMR. Furthermore, it was decided not to decrease the operational temperature beyond -90°C to avoid the possibility of sample freezing.

TABLE 18. Arrhenius Activation Energies for the Aldol Addition of **4** to **5a** Promoted by **7a** As Determined by RINMR Analysis^a

activation parameters	activation values
ΔH^\ddagger (kcal mol ⁻¹)	1.5 ± 0.5
ΔS^\ddagger (cal mol ⁻¹ K ⁻¹)	-51.9 ± 1.0
ΔG^\ddagger (kcal mol ⁻¹)	17.3 ± 1.0

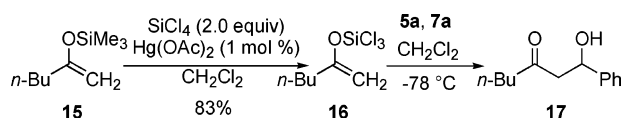
^a Activation parameters were calculated for $T = 303\text{ K}$.

2.7. Determination of the Turnover-Limiting Step. Through extensive kinetics studies using GC, IR, and NMR analysis, the molecularity for the Lewis base catalyzed aldol addition

(27) For examples on the use of rapid injection NMR techniques, see: (a) McGarrity, J. F.; Prodolliet, J.; Smyth, T. *Org. Magn. Reson.* **1981**, *17*, 59–65. (b) Palmer, C. A.; Ogle, C. A.; Arnett, E. M. *J. Am. Chem. Soc.* **1992**, *114*, 5619–5625. (c) Reetz, M. T.; Raguse, B.; Marth, C. F.; Hügel, H. M.; Bach, T.; Fox, D. N. A. *Tetrahedron* **1992**, *48*, 5731–5742. (d) For an in depth discussion of the design, construction and application of the RINMR apparatus, see ref 10b.

involving trichlorosilyl enolates has been elucidated and shows a rate expression as $\text{rate} = k[\text{cat}][\text{enolate}][\text{aldehyde}]$ for catalyst **7j** and $\text{rate} = k[\text{cat}]^2[\text{enolate}][\text{aldehyde}]$ for catalyst **7a**. Although the order of each component at the rate-determining step is known, either complexation or aldolization is turnover limiting. The experimentally determined reaction order is consistent with both scenarios, and while the Arrhenius activation parameters may suggest complexation is turnover limiting (large negative ΔS^\ddagger , small ΔH^\ddagger), it does not discount aldolization for this event. To conclusively determine the turnover-limiting step, kinetic isotope effects (KIE) from natural-abundance ^{13}C NMR analysis (as pioneered by Singleton)²⁸ were utilized.²⁸ Because the formation of diastereomers would be readily evident in the analysis required for natural abundance kinetic KIE using NMR spectroscopy, a methyl ketone enolate was chosen to simplify the kinetic analysis. 2-Hexanone trichlorosilyl enolate, **16**, was selected for its reactivity and ease of preparation,¹² Scheme 7.

SCHEME 7



Fortunately, ^{13}C NMR analysis of the aldol product between enolate **16** and **5a** at 5% conversion afforded excellent results. To obtain sufficient material for ^{13}C NMR analysis, the aldol addition was performed on a 10 mmol scale and was stopped at 5% conversion by using only 0.05 equiv of benzaldehyde with respect to trichlorosilyl enolate. To corroborate the results, an additional reaction was performed using 0.05 equiv of enolate with respect to benzaldehyde. The product from each reaction was isolated and purified in a manner similar to all preparative-type reactions. The results from a reaction that was stopped at 5% conversion were compared with those from a standard reaction taken to full conversion. The integration ratios are shown in parts a and c of Figure 10 and reveal a depletion in the ^{13}C isotope at the reactive center of the excess reagent in both cases. The KIEs²⁹ are shown in parts b and d of Figure 10 and clearly show a KIE at the reactive trichlorosilyl enolate carbon and the reactive aldehydic center.

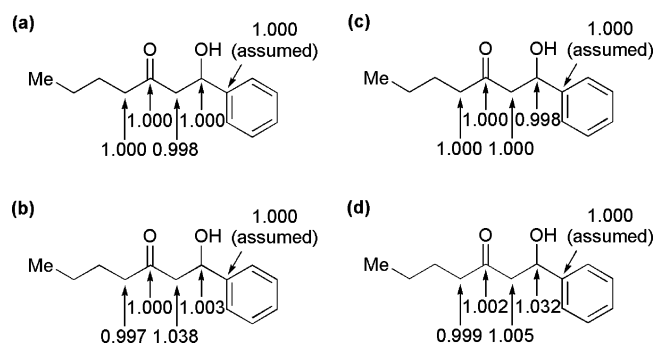


FIGURE 10. (a) ^{13}C isotopic composition of aldol adduct **17** isolated from a reaction taken to 5% conversion using limited aldehyde. (b) ^{13}C KIEs ($k^{12}\text{C}/k^{13}\text{C}$) for a reaction taken to 5% conversion using limited aldehyde. (c) ^{13}C isotopic composition of aldol adduct **17** isolated from a reaction taken to 5% conversion using limited enol ether. (d) ^{13}C KIEs ($k^{12}\text{C}/k^{13}\text{C}$) for a reaction taken to 5% conversion using limited enol ether.

Discussion

1. Unpromoted Reaction. By employing pseudo-first order conditions, the molecularity for the unpromoted aldol addition was determined to be first order in both trichlorosilyl enolate and aldehyde. This affords the classic bimolecular rate expression of $d[\text{product}]/dt = k[\text{enolate}][\text{aldehyde}]$. A combination of the molecularity and the stereoregularity for the uncatalyzed reaction allows the reasonable hypothesis that aldolization occurs through a pentacoordinate silicon species whose ligands are arranged in a trigonal bipyramidal manner, Figure 11. For intramolecular addition to take place, the aldehyde and the enol oxygen must be in an apical/basal cis configuration. Two such diastereomeric complexes are possible; in the more stable (ii), the aldehyde occupies the apical position with a chloride occupying the remaining one. Thus the two remaining chlorides and the enol ether would be positioned around the basal plane. However, this is not the more reactive of the two. For the components to be activated in the absence of catalyst, a pseudorotation to place the aldehyde in a basal position (sp^2) and the enol ether in an apical position (3-center-4-electron hybrid) is necessary (iii).³⁰

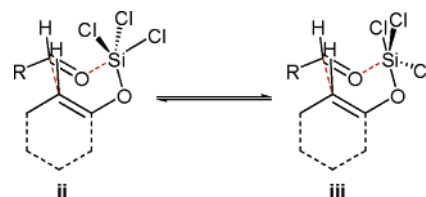


FIGURE 11. Pentacoordinate silicon in an uncatalyzed reaction.

The Arrhenius parameters for the unpromoted aldol addition revealed ΔG^\ddagger to be primarily a function of ΔS^\ddagger , whereas ΔH^\ddagger was a minor contributor. Such a large negative ΔS^\ddagger is typically indicative of a highly organized transition structure or an unfavorable preequilibrium.³¹ Stereochemical studies implicate a boatlike transition structure as dictated by the correlation of (*E*)-enolate \rightarrow *syn*-aldolate and (*Z*)-enolate \rightarrow *anti*-aldolate. Although the closed nature of the transition structure certainly contributes to the ΔS^\ddagger it is unlikely that rotational and vibrational degrees of freedom could alone afford such large negative entropies of activation. It is therefore likely that complexation of the aldehyde to the trichlorosilyl enolate is an independent and reversible step toward aldolization. Furthermore, a surprisingly small ΔH^\ddagger is suggestive of a high level of activation in this binary complex. This conclusion is understandable considering the rate at which the trichlorosilyl enolates react with aldehydes at room temperature.

(28) Singleton, D. A.; Thomas, A. A. *J. Am. Chem. Soc.* **1995**, *117*, 9357–2358.

(29) For a detailed discussion involving the determination of ^{13}C KIEs from NMR integrations and error analysis, see ref 28.

(30) The trigonal bipyramidal silicon structure is created from one hypervalent (3-center-4-electron) hybrid orbital and three sp^2 hybrids (basal plane). The enolate will experience the greatest activation in the apical position because of the concentration of electron density at the ligands in hypervalent bonds. Correspondingly, the aldehyde will experience the greatest activation in the basal position because the sp^2 orbitals have the most s-character and therefore are the most electronegative sites. For a description of this bonding scheme, see: Curnow, O. J. *J. Chem. Educ.* **1998**, *75*, 910–915.

(31) For additional examples of kinetic studies on aldol additions, see: (a) Myers, A. G.; Widdowson, K. L. *J. Am. Chem. Soc.* **1990**, *112*, 9672–9674. (b) Myers, A. G.; Widdowson, K. L.; Kukkola, P. J. *J. Am. Chem. Soc.* **1992**, *114*, 2765–2767. For an ab initio MO study, see: (c) Gung, B. W.; Zhu, Z.; Fouch, R. A. *J. Org. Chem.* **1995**, *60*, 2860–2864.

2. Promoted Reaction. 2.1. Kinetics. The discovery of primary ^{13}C KIEs under conditions of limiting reagents leaves little doubt that the turnover limiting step can only be aldolization following assembly of the reactive complex. If complexation were turnover limiting, then no ^{13}C KIE would be observed in the natural abundance ^{13}C NMR studies, because no isotopic partitioning for carbon is expected during this associative step. The observance of a KIE greater than 1 for $k^{12}\text{C}/k^{13}\text{C}$ is consistent with the manner in which the experiment was established. The use of excess trichlorosilyl enolate allows for preferential aldol addition of the ^{12}C enolate, enriching the amount of ^{12}C in the isolated aldol adduct. The result observed by ^{13}C NMR is a decrease in relative area at the reactive carbon, and ultimately a primary KIE value greater than 1.0. Furthermore, it is unlikely that a primary KIE would be observed should the rate-limiting step have been the complexation of ligands or even catalyst turnover.

The use of in-situ monitoring using ReactIR to study promoted reactions proved to be invaluable compared to traditional GC analysis. Determining the change in the observed rate constant (k_{obs}) as a function of catalyst concentration readily established that promoted aldol additions are first order dependent on catalyst **7j** ($m = 1.014$). This behavior provided direct evidence for the presence of a single catalyst molecule in the transition structure when a bulky phosphoramidate is employed. The fact that the value for the slope is nearly one also suggests that little if any product yielding side reactions occur, of which, the most important is the background, or catalyst free reaction. Certainly, if this were significant, the value of the logarithmic relationship would most likely be much less than one to account for reactions proceeding in the absence of phosphoramidate. Additionally, should the 2:1 catalyst/enolate pathway be competitive, a value between 1 and 2 would be expected depending upon the kinetic competition between the 1:1 and 2:1 pathways. A slope close to 1.0 clearly shows no product-yielding side reactions are competitive, and thus, all products arise from a single, kinetically competent pathway.

As in the unpromoted aldol addition, the Arrhenius activation parameters determined using phosphoramidate **7j** show that ΔG^\ddagger is again dominated by ΔS^\ddagger and even less so by ΔH^\ddagger . The nearly vanishing ΔH^\ddagger is indicative of the greater activation in the phosphoramidate-promoted complex compared to the unpromoted complex. Once again the large negative ΔS^\ddagger suggests reversible preassembly of the activated complex involving enolate, aldehyde and phosphoramidate prior to aldolization.

The challenges of determining kinetic parameters for relatively fast reactions at subambient temperatures were greatly overcome by the use of RINMR spectroscopy. The apparatus was crucial for providing meaningful, real-time kinetics of reactions with half-lives on the order of tens of seconds. Measurement of k_{obs} as a function of the concentration revealed second order dependence in phosphoramidate **7a**. Although previous experimental results have suggested mechanistic differences, this provided the first direct evidence for the existence of a mechanistic dichotomy between catalysts **7a** and **7j**, namely that reactions using **7a** proceed through a two-phosphoramidate pathway whereas reactions using **7j** proceed through a one-phosphoramidate pathway. Additionally, a two phosphoramidate mechanism provides unambiguous substantiation for a ligand effect as the origin of nonlinear asymmetric induction observed for **7a**.

The activation energies for a reaction using phosphoramidate **7a** are representative of what has been observed for the previous reaction sets. Again, the large negative value for ΔS^\ddagger implies an unfavorable preequilibrium, although ΔS^\ddagger is notably smaller for reactions catalyzed by phosphoramidate **7a** than for the previous two examples. This is striking considering assembly of the activated complex involves coordination of four independent species. The fact that ΔS^\ddagger is smaller may be the effect of solvation or other interactions with the reaction medium. In any case, this two-phosphoramidate complex is more kinetically competent than the single phosphoramidate complex. This translates into a lower ΔG^\ddagger and ultimately into faster reaction rates as compared to the more bulky phosphoramidate **7j**, Figure 12.

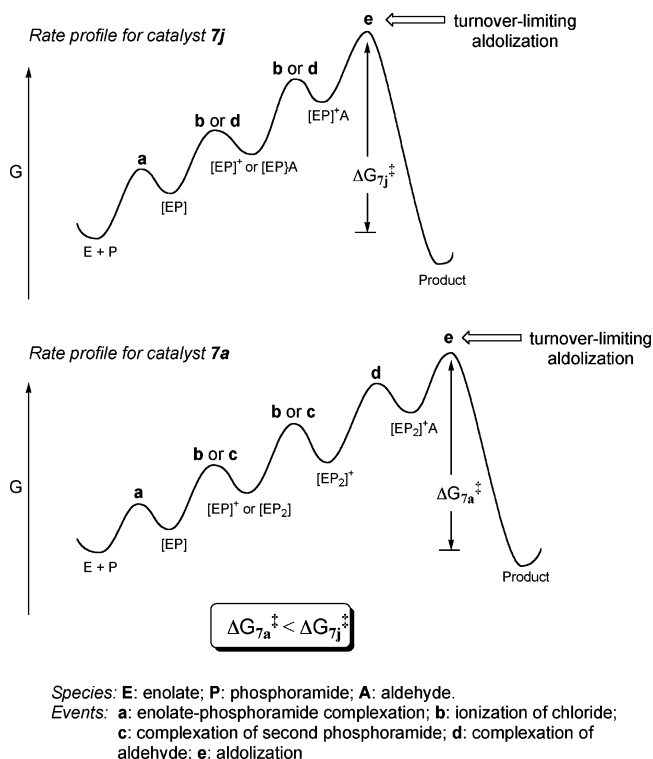


FIGURE 12. Free energy profiles for aldol additions using phosphoramidate **7j** and **7a**.

2.2. Overview of Chemical Results. The remarkable rate acceleration observed when reactions are performed in the presence of phosphoramidates is clearly the basis for the high level of stereoselection observed with specific phosphoramidates. It is of no surprise that the level of enantioselectivity is proportional to the activity of the catalyst. It is also noteworthy to recognize that the direction of stereoselection is tunable based upon the structure of the phosphoramidate. With regard to *E*-trichlorosilyl enolates (such as **4**), bulky phosphoramidates such as **7j** and **7k** are selective for the *syn* aldol adduct, *E*→*syn*, through a one-phosphoramidate pathway. Conversely, smaller phosphoramidates such as **7a** and **7m** are selective in the *anti* manifold, *E*→*anti*, via a two phosphoramidate pathway. Although any modifications around the phosphoramidate structure will likely affect a change in reactivity and stereoselectivity, it is predominantly the substituents on the nitrogens of the diazaphospholidine skeleton that determine the relative bulk of the catalyst. Specifically, methyl and ethyl substituents are considered small whereas aryl substituents such as phenyl and 1-naphthyl may be considered large on the basis of the previous analysis.

In addition to the shape of the phosphoramidate, the amount of the catalyst also has a profound effect on stereoselectivity. Again considering (*E*)-trichlorosilyl enolates, decreasing the loading of catalyst generally increases formation of the syn isomer by promoting the one-phosphoramidate pathway. To enhance the anti manifold, higher loadings of phosphoramidates may be required which activate the two-phosphoramidate pathway. Indeed this was also achieved by slow addition of the aldehyde component. In this manner, the relative concentration of the phosphoramidate catalyst remained high with respect to the reactive partners allowing reactions to proceed through the more selective two-phosphoramidate mechanism. Although subtle, this unexpected loading effect illustrates the mechanistic dichotomy for various phosphoramidates (*vide supra*).

Perhaps a more striking detail regarding the stereochemical effects of different phosphoramidates lies in the remarkable difference between **7a** (*dimethylstilbene*-1,2-diamine) and **7j** (*diphenylstilbene*-1,2-diamine) with regard to the diastereoselectivity. As clearly highlighted in the nonlinear effect studies, **7a** displays a positive nonlinear effect allowing stereochemical inductions greater than the actual enantiopurity of the catalyst used. Subsequent studies have ruled out product inhibition, and a reservoir effect and indeed kinetic studies have defined a multiple ligand model as the basis for nonlinear induction. Conversely, **7j** displayed linear induction, proceeding through a one-phosphoramidate pathway as determined by kinetic studies.

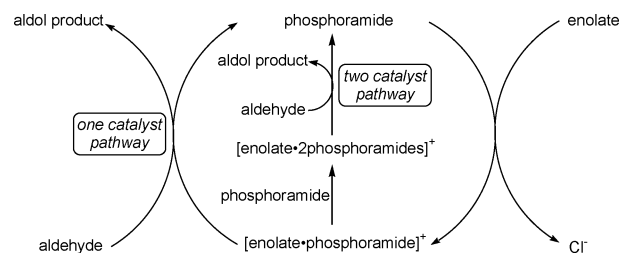
The ability of various ionic additives such as tetrabutylammonium chloride ($\text{Bu}_4\text{N}^+\text{Cl}^-$) and tetrabutylammonium triflate ($\text{Bu}_4\text{N}^+\text{OTf}^-$) to affect the rates of reaction underscores the nature of the silicon center during phosphoramidate-catalyzed aldol additions of trichlorosilyl enolates to aldehydes. Attenuation of rate from the addition of $\text{Bu}_4\text{N}^+\text{Cl}^-$ is indicative of a common ion effect,³² suggesting reactions proceed through a cationic intermediate created by the dissociation of chloride.³³ The addition of $\text{Bu}_4\text{N}^+\text{OTf}^-$ enhances the ionic strength of the medium allowing stabilization of the ionic intermediates and thus provides a rate acceleration resulting in an increased conversion from 44% to 92% after only 8 min.³⁴

The addition of Brønsted acids greatly increased the syn selectivity for the addition of cyclohexanone-derived enolate **4** to benzaldehyde for both achiral and chiral phosphoramidates. The origin of this effect is not certain, but most likely arises from an enhancement in the reaction flux through the one-phosphoramidate pathway (*E*→*syn*). Because this effect was most pronounced at low catalyst loading, it is possible that the Brønsted acids function to remove a fraction of catalyst from the trichlorosilyl enolate binding equilibrium by protonation of the oxygen, although their pK_a 's are not low enough. Alternatively, the Brønsted acids may interact with the trichlorosilyl enolates to form chlorosilylcarboxylates and HCl which can

protonate the phosphoramidate. Interestingly, the strongest acid, triflic acid, completely suppressed the catalyzed pathway, and only background reaction was observed.

2.3. Mechanistic Hypothesis. Kinetic analysis has revealed that a mechanistic dichotomy exists between the reactions catalyzed by phosphoramidates **7a** and **7j**. Under typical loadings (5–15 mol %), phosphoramidate **7j** catalyzes the aldol addition of trichlorosilyl enolates to aldehydes through the coordination of a single phosphoramidate. Alternatively, **7a** acts through a two-phosphoramidate mechanism. Furthermore, results taken from the salt effect studies would imply that aldol addition proceeds through a cationic silicon species created by the coordination of one or two phosphoramidates and the subsequent ionization of chloride. It is likely that coordination of an aldehyde to this cationic siliconate activates it toward enolate addition, Scheme 8.

SCHEME 8



3. Integration of Results. The most influential component in the rate of the aldol addition of trichlorosilyl enolates to aldehydes is the structure of the phosphoramidate. A survey of various substituents at different locations around the phosphoramidate revealed that large substituents on the nitrogens of the 2,5-diazaphospholidine skeleton greatly attenuated the rate of aldolization. For the addition of **4** to benzaldehyde, yields diminished to 31% when using the naphthyl-substituted phosphoramidate **7k**. Even the use of stoichiometric amounts of this phosphoramidate could only enhance yields to 52%. Similar results were observed for the achiral phosphoramidates. Although for some aldol partners, use of the naphthyl-substituted achiral catalyst **11c** showed only minimal rate attenuation compared to **11a**, use of a branched aliphatic group in **11b** afforded products in only 35% yields. Unlike the nitrogen substituents on the diazaphospholidine ring, modification of the chiral backbone of the phosphoramidates had only a modest effect on rates and selectivities of reactions. Although yields were lower when employing the bulky naphthyl phosphoramidates such as **7f** and **7g**, the overall effect was minimal when compared to effects from substitution at the phospholidine nitrogens. Moreover, the addition of electron-withdrawing and electron-donating groups on the phenyl rings did not have a major effect on the rate of addition. Moving away from the aryl-based backbone to the cyclohexyldiamine-derived phosphoramidate **7e** led to the largest rate decrease. Last, modification of the substituents on the external nitrogen of the chiral phosphoramidates had little effect on the rate of addition of **4** to benzaldehyde. However, a pronounced effect was observed when employing enolate **9**. Contracting the piperidinyll substituent to a pyrrolidinyll unit caused yields to drop significantly from 77% to 41% for phosphoramidates **7a** and **7q**, respectively. Taken together, these results reveal that bulky substituents on the nitrogen atoms of the phospholidine ring reduce the propensity for multiple phosphoramidate coordination forcing reactions through the slower acting one-phosphoramidate pathway.

(32) (a) Bateman, L. C.; Hughes, E. D.; Ingold, C. K. *J. Chem. Soc.* **1940**, 974, 1017–1029. (b) Streitwieser, A. *Solvolytic Displacement Reactions*; McGraw-Hill: New York, 1962. (c) Thornton, E. *Solvolysis Mechanisms*; Ronald Press: New York, 1964.

(33) Cationic silicon species have been proposed as intermediates in other Lewis base promoted reactions; see refs 3b, 4, 11a, 25, and: (a) Chojnowski, J.; Cypriak, M.; Michalski, J.; Wozniak, L. *J. Organomet. Chem.* **1985**, 288, 275–282. (b) Corriu, R. J. P.; Dabosi, G.; Martineau, M. *J. Organomet. Chem.* **1980**, 186, 25–37. (c) Bassindale, A. R.; Lau, J. C.-Y.; Taylor, P. G. *J. Organomet. Chem.* **1995**, 490, 75–82. (d) Bassindale, A. R.; Lau, J. C.-Y.; Taylor, P. G. *J. Organomet. Chem.* **1995**, 499, 137–141.

(34) A similar effect has been noted for $\text{Bu}_4\text{N}^+\text{I}^-$ (ref 25). This observation also rules out the possibility that the retarding effect of $\text{Bu}_4\text{N}^+\text{Cl}^-$ arises from the role of chloride as a competitive ligand for the complex.

Another significant influence on the rate of reaction was the effect of salt additives. As discussed previously, $\text{Bu}_4\text{N}^+\text{OTf}^-$ accelerated the addition of **4** to **5a** in the presence of **7j**. This was interpreted as stabilization of ionic intermediates on the mechanistic pathway arising from the enhanced ionic strength of the medium. Furthermore, the decrease in rate from the addition of $\text{Bu}_4\text{N}^+\text{Cl}^-$ suggests not only the intermediacy of ionic intermediates but also that cationic siliconates arise from the ionization of chloride. The common ion effect certainly implicates chloride as a key participant in the aldol addition of trichlorosilyl enolates to aldehydes and also explains the low reactivity of aliphatic aldehydes by chlorosilyl ether formation.⁸

The use of geometrically defined enolates such as **4** and (Z)-**9** allows for additional mechanistic insights based on the resulting stereochemical outcomes. The stereochemical correlation shows that the addition proceeds through a closed transition structure centered around a siliconium ion. This stems from the observation that a switch in syn-anti manifolds occurs when employing either **4** or (Z)-**9** in aldol additions using similar phosphoramides. The switch in diastereoselectivity can best be explained from configurational correlation via aldol additions through closed transition structures.³⁵ In the case of enolate **4**, this would imply addition through a boatlike transition structure to give syn aldol products in the presence of catalysts such as **7j** (diphenylstilbene-1,2-diamine). Likewise, anti products would arise from additions through a chairlike transition structure from catalysts similar to **7a** (dimethylstilbene-1,2-diamine).

Together with kinetic studies, the stereochemical information from the addition of geometrically defined enolates allows a clearer mechanistic picture to emerge. For phosphoramide **7j**, kinetic and nonlinear effect studies revealed that a single phosphoramide is present in the transition structure for the stereochemical-determining step. Because this phosphoramide affords syn products from *E*-enolates, it follows that **7j** acts in a 1:1 manner with trichlorosilyl enolates to afford aldol products through a *boatlike* transition structure. As is the case for other syn-selective phosphoramides such as **7k** and **7p**, steric bulk proximal to the coordinating oxygen limits complexation to a 1:1 mode with aldolization proceeding through a boatlike transition structure.^{11a}

For the less bulky phosphoramide **7a**, kinetic and nonlinear effect studies revealed the aldol additions were second order in catalyst, clearly implicating a transition structure containing two phosphoramides for the stereochemistry determining step in the aldol addition. Additionally, the stereochemical consequences would dictate that aldol addition through this 2:1 (phosphoramide/silicon) pathway proceeds via a chairlike structure to afford anti products from enolate **4**. Indeed, unlike the more sterically congested catalysts, phosphoramides bearing small substituents on the internal nitrogens are able to achieve 2:1 complexation.^{11a} This divergence in mechanism is further highlighted by the remarkable loading effect observed for the diastereoselectivity of aldol additions in the presence **11c**. At low catalyst loadings where 1:1 complexation is most likely, the reactions are highly syn selective with enolate **4** and catalyst **11c**. Increasing the amount of phosphoramide up to 2.0 equiv allows the 2:1 pathway to become competitive, affording greater

amounts of the anti product. Moreover, the observation that slow addition of the aldehyde leads to enhanced anti diastereoselectivity from the reaction of **4** with **5a** in the presence of **7a** demonstrates that by maintaining a relatively high concentration of catalyst with respect to available substrates, aldol addition proceeds predominantly by a 2:1 pathway, through a chairlike transition structure.

The preference for the 1:1 or 2:1 (phosphoramide/silicon) complexes to adopt either boatlike or chairlike transition structures is likely controlled by the nature of the two different silicon complexes. As in the unpromoted pathway, the 1:1 manifold involves five ligands positioned in a trigonal bipyramidal manner around the now cationic silicon center (Figure 13). As before, the components must be proximal for reaction to occur and it is likely that in the more stable complexes, the aldehyde occupies one of the apical positions and either the phosphoramide or one of the chlorides in the other. On the basis of X-ray crystallographic studies of five-coordinate silicon³⁶ and tin complexes,^{11a,37} we suspect that the phosphoramide occupies the apical position, leaving the enol ether and the two chlorides to orient along the basal plane. This positions the enolate and phosphoramide in relatively close proximity to the aldehyde, **iv**. A more reactive complex would arise from a Berry pseudorotation that interchanges the enolate and aldehyde moieties, **v**.³⁰ In either of these complexes, the preference for the boat geometry is rooted in the small bond angle at silicon (90°) and the placement of the hydrogens on both the aldehyde carbonyl group and the *E*-enolate toward the chlorine atom. In any chairlike arrangement, either the aldehyde residue or the enolate spectator group will experience unfavorable steric interactions.

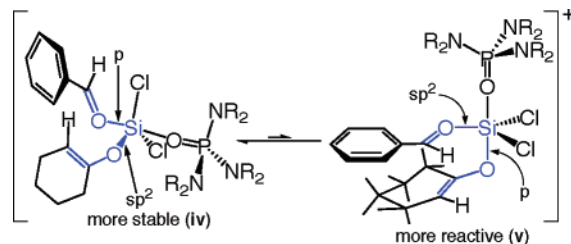


FIGURE 13. Isomeric 1:1 cationic complexes.

In the 2:1 pathway, the cationic siliconate must now adopt an octahedral geometry to accommodate the additional phosphoramide ligand. Although multiple isomeric complexes are possible, the aldehyde and enolate must be bound in a *cis*-manner for reaction to take place (Figure 14). This factor reduces the number of geometrically isomeric complexes to four: three with *cis*-configured phosphoramides (**vi**–**viii**) and one with *trans*-configured groups (**ix**).³⁸ Although we are unable to unequivocally identify which or how many of these complexes contribute to the overall reaction flux, several factors allow qualitative conclusions. First, given the high enantioselectivity observed with **7a** it is unlikely that multiple complexes

(35) (a) Evans, D. A.; Nelson, J. V.; Taber, T. R. In *Topics in Stereochemistry*; Eliel, E. L., Wilen, S. H., Eds.; Wiley-Interscience: New York, 1982; Vol. 13, Chapter 1. (b) Braun, M. In *Stereoselective Synthesis, Methods of Organic Chemistry (Houben-Weyl)*, E21 ed.; Helmchen, G., Hoffman, R., Mulzer, J., Schaumann, E., Eds.; Thieme: Stuttgart, 1996; Vol. 3; pp 1603–1612.

(36) Reviews on hypercoordinate silicon compounds: (a) Kost, D.; Kalikhman, I. In *The Chemistry of Organic Silicon Compounds*; Rappoport, Z., Apeloig, Y., Eds.; Wiley: Chichester, 1998; Vol. 2, Part 2. (b) Holmes, R. R. *Chem. Rev.* **1996**, *96*, 927–950. (c) Chuit, C.; Corriu, R. J. P.; Reye, C.; Young, J. C. *Chem. Rev.* **1993**, *93*, 1371–1448. (d) Tandura, S. N.; Voronkov, M. G.; Alekseev, N. V. *Top. Curr. Chem.* **1986**, *131*, 99–189.

(37) Aslanov, L. A.; Attiya, V. M.; Ionov, V. M.; Permin, A. B.; Petrosyan, V. S. *Zh. Strukt. Khim.* **1977**, *18*, 1113–1118.

(38) Complexes **vi** and **vii** also exist as two limiting diastereomeric chair complexes, but will not be considered at this level of analysis.

contribute similarly. Moreover, recent computational analysis of the transition structures for a trichlorosilyl ketene acetal reacting with a ketone under catalysis by a bis-pyridine *N*-oxide suggests that complexes that orient the carbonyl oxygen trans to a chlorine atom are not stable relative to those with trans carbonyl-ligand geometries.³⁹ Thus, complexes **vi** and **ix** are disregarded.⁴⁰ Of the two remaining complexes, **vii** is expected to be more reactive because the enolate participates in 3-center-4-electron bonding with the chlorine rendering it more nucleophilic, whereas the aldehyde participates in bonding via an sp hybrid which activates by electron withdrawal.

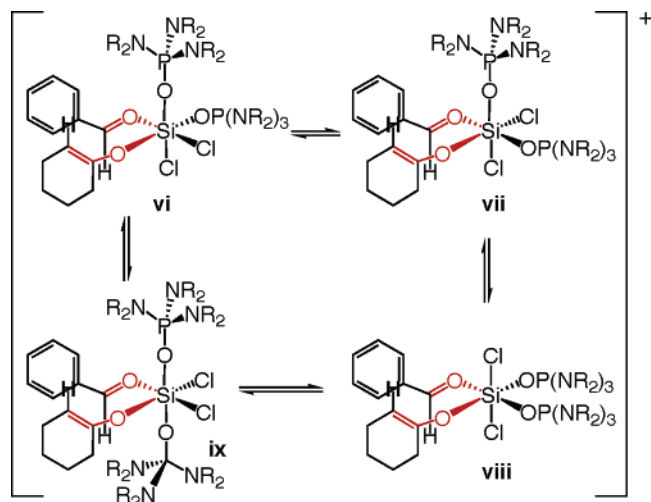


FIGURE 14. Isomeric 2:1 cationic complexes.

Although both the 1:1 and 2:1 manifolds afford aldol products with high diastereoselectivities, higher enantioselectivities are generally observed through the 2:1 complex. The improved enantioselectivities may in part arise from the increased reactivity of the 2:1 pathway, causing the background reaction to be less competitive. The enhanced reactivity of the 2:1 complex over the 1:1 complex may stem from an increased activation of the aldehyde component in the octahedral complex compared to the trigonal bipyramidal complex (tbp). The increased s-character in the aldehyde–silicon bond of the octahedral complex (sp hybrid) versus the sp² hybrid in the tbp complex can lead to greater electrophilic activation. Additionally, the 2:1 or 6-coordinate complex is better able to impart stereochemical information by creating a more dissymmetric space around the reactive partners compared to a 1:1 complex.

The aryl groups in the stilbene-1,2-diamine phosphoramidate backbone afforded the highest enantioselectivities (Table 5). By switching to an aliphatic backbone such as cyclohexane-1,2-diamine, **7e**, enantioselectivities deteriorated. Although electronic variations imparted little effect on rates of aldol additions, their effect on stereoselectivity is more pronounced. Electron-withdrawing groups such as the *p*-trifluoromethyl substituents in **7b** had a detrimental effect on the diastereoselectivity for the addition of **4** to benzaldehyde. In addition, the enantioselectivity was attenuated as well, though not to the same degree.

(39) The octahedral silicon structure is created from two hypervalent (3-center-4-electron) hybrid orbitals and one sp hybrid. For a description of this bonding scheme, see refs 9c and 30.

(40) The high tendency of group 14 complexes to be cis configured also rules out complex **ix**. Ruzicka, S. J.; Merbach, A. E. *Inorg. Chim. Acta* **1976**, *20*, 221–229.

Unlike electron-withdrawing groups, electron-donating groups such as the *p*-methoxy substituents in **7c** had little effect on the stereochemical course of reaction. Both the diastereo- and enantioselectivities remained high as compared to the parent phosphoramidate. Surprisingly, the use 3,5-dimethylphenylstilbenediamine as the chiral backbone in **7d**, afforded aldol products with attenuated stereoselectivity. The origin of these somewhat subtle effects is unclear and must await a detailed computational analysis of the reaction pathways.

As with modifications to the chiral backbone, substitutions at the external nitrogen greatly effect stereoselectivities. Indeed, only the small *N,N'*-dimethyl substituents (**7m**) and the piperidinyll group (**7a**) afforded high enantioselectivities for reactions of **4** to benzaldehyde. Introducing larger substituents such as isopropyl (**7p**), *n*-propyl (**7n**), or phenyl groups (**7q**) greatly diminished enantioselectivities. In fact, these modifications led to an inversion in diastereoselectivity to the syn manifold, suggesting that reaction now proceeds through a 1:1 pathway. Even the removal of a single methylene unit from the piperidinyll ring to afford a pyrrolidinyll-substituted phosphoramidate (**7q**) resulted in attenuated stereoselectivities. Although the individual effects of substitutions around the phosphoramidate structure are not always predictable, it is clear that a delicate balance is necessary to achieve high stereoselectivities.

Taken together, the chemical and kinetic (and spectroscopic) results provide a unified mechanism to be formulated for the phosphoramidate-catalyzed aldol additions of trichlorosilyl enolates, Figure 15. Although the kinetic data clearly indicate aldolization to be turnover limiting the experimental results cannot adequately predict the order of events prior to aldol addition. Initial complexation between enolate **4** and a phosphoramidate can generate the activated siliconium intermediate **x**.⁴¹ With bulky phosphoramidates such as **7j** or at low catalyst loading, the intermediate **x** directly binds the aldehyde substrate and then reacts via a cationic trigonal bipyramidal complex (e.g., **v**) in a boat conformation to afford the syn aldol product. Although the enantioselectivities are only modest, the major enantiomer consistently arises from attack on the *Si* face of the enolate when using the (*S,S*)-**7j** catalyst. With smaller phosphoramidates, such as **7a**, or at higher catalyst loadings, **x** can bind a second molecule of phosphoramidate to form a new siliconium intermediate **xi**. This species retains sufficient electrophilicity to bind the substrate aldehyde and then react via a cationic octahedral complex (e.g., **vii**) in a chair conformation to afford the anti aldol product. In this manifold, the enantioselectivities are much higher, but again the major enantiomer arises from attack on the *Si* face of the enolate with the (*S,S*)-**7a** catalyst. Thus, the dramatic change in diastereoselectivity results from a change in the preference for reaction via a chair versus a boat transition structure which in turn arises

(41) We cannot exclude the existence of a preassociation between trichlorosilyl enolate and the aldehyde. Considering the spontaneity of the uncatalyzed reaction at ambient temperatures, this association certainly takes place albeit with greatly diminished consequences at -78°C . Moreover, as illustrated in Figure 12, we cannot rule out association of a second ligand prior to ionization of the chloride. Species **x** is a highly reactive tetravalent siliconium ion and may not be formed without a second ligand. In the case of the one-phosphoramidate pathway, ionization would occur after aldehyde binding but prior to aldolization and would be needed for activation of the aldehyde through a cationic species. In the two-phosphoramidate pathway, the ionization would occur after the binding of the second phosphoramidate, also shown in Figure 15. In both of these cases, the silicon atom would always be Lewis-satisfied (i.e., in $[\text{EL}_2]^+$ the silicon has a half share of 9 electrons). It never has to become a very high energy cationic 7 electron species and remains hypervalent and formally electron rich.

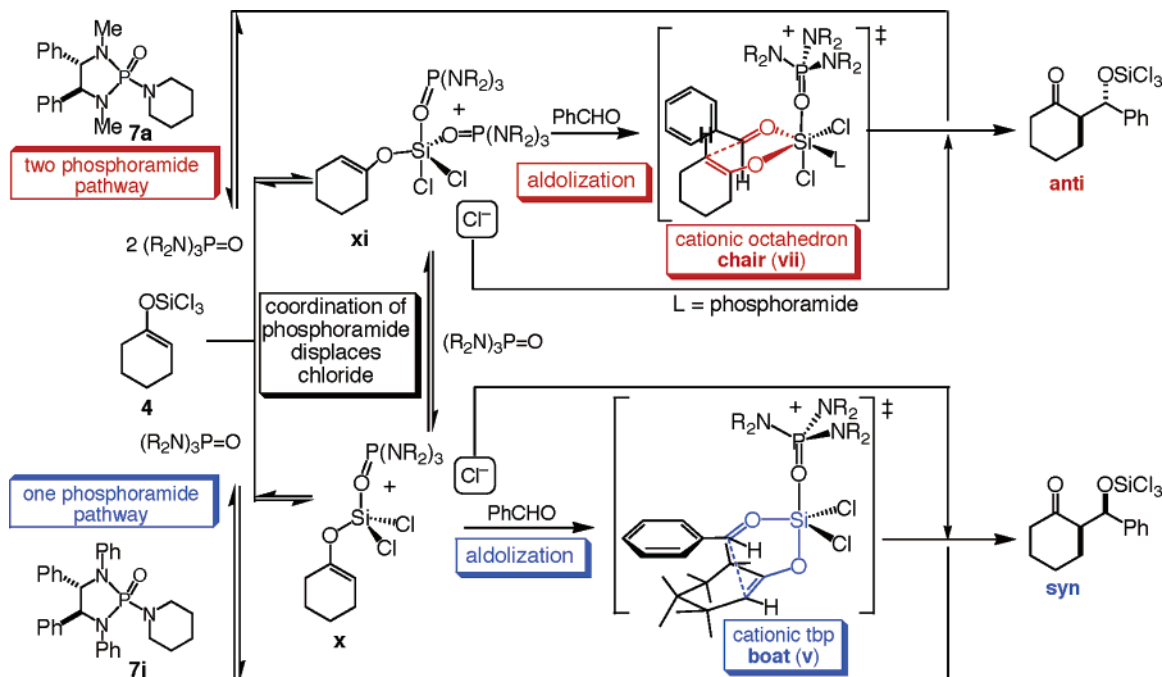


FIGURE 15. Grand unified mechanistic scheme for phosphoramidate-catalyzed aldolization.

from a change in the structure of the siliconium complex, itself a consequence of the size of the phosphoramidate ligand. The origin of the preference for a chairlike transition structure in the octahedral complexes remains obscure and will require computational analysis.

Conclusions and Outlook

We have developed a mechanistic rationale to explain the origin of rate enhancements and mode of stereoselectivity for the phosphoramidate-catalyzed aldol additions of trichlorosilyl enolates to aldehydes. Structure–activity–selectivity relationships were developed for a variety of phosphoramidates detailing the propensity for bulky phosphoramidates to participate via a 1:1 phosphoramidate/enolate pathway through boatlike transition structures centered around a 5-coordinate cationic siliconate. Likewise, smaller phosphoramidates are able to engage the trichlorosilyl enolate in a 2:1 manner, reacting through 6-coordinate, chairlike transition structure. The mechanistic interpretation fully explains the remarkable loading effects and nonlinear effects observed.

Clearly, the operation of dual mechanistic pathways that are dependent on catalyst size and concentration present significant preparative problems. The less selective 1:1 pathway will intervene as catalyst loading drops (to improve turnover) or as catalyst size increases (to improve enantioselectivity). The obvious solution is to covalently tether two catalyst molecules and study the cooperativity of the two subunits. This strategy has yielded excellent results for enantioselective allylation^{3b,11b} and for reactions promoted by silicon tetrachloride.²⁵ Initial studies in this direction for aldolization are promising, and further refinements and improvements will be reported in due course.⁴²

(42) We have demonstrated a cooperative effect on the stereoselectivity of aldol additions with acyclic trichlorosilyl enolates using tethered phosphoramidates: see ref 6b.

Experimental Section

General Experimental Procedures. See the Supporting Information.

General Procedure for Catalyzed Aldol Additions of Trichlorosilyl Enolates 4 and (Z)-9 with Fast Addition of Aldehyde: (–)-(2*R*,1′*S*)-2-(Hydroxyphenylmethyl)cyclohexanone (*anti*-6a). Catalyst (*S,S*)-7a (7.3 mg, 0.02 mmol, 0.1 equiv) was dissolved in CH₂Cl₂ (2 mL) and was cooled to –78 °C. Trichlorosilyl enolate 4b (40 μL, 0.22 mmol, 1.1 equiv) was added dropwise over 1 min. Benzaldehyde (20.3 μL, 1.0 mmol) was then added neat, over 20 s. The reaction mixture was stirred at –78 °C for 2 h, satd aq NaHCO₃ solution (5 mL) was added quickly, and the mixture was allowed to warm to rt. The phases were separated, and the aqueous phase was extracted with CH₂Cl₂ (3 × 10 mL). The organic phases were combined, dried over Na₂SO₄, filtered, and concentrated in vacuo. The syn/anti ratio was determined by ¹H NMR (400 MHz) analysis to be 1/28. The crude material was purified by column chromatography (SiO₂, hexane/EtOAc, 6/1) to give 1.3 mg of (–)-syn-6a as an oil and 35.3 mg (90% total) of (–)-anti-6a as a clear oil. Analytical data for (–)-anti-6a: mp 41–42 °C; ¹H NMR (400 MHz, CDCl₃) 7.36–7.26 (m, 5 H, Ph), 4.78 (dd, *J* = 9.2 and 2.4, 1 H, PhCHOH), 3.98 (d, *J* = 2.4, 1 H, OH), 2.64–2.58 (m, 1 H, C(2)_{H_{ax}}), 2.50–2.44 (m, 1 H, C(6)_{H_{eq}}), 2.39–2.31 (m, 1 H, C(6)-H_{ax}), 2.11–2.03 (m, 1 H, C(5)_{H_{eq}}), 1.80–1.74 (m, 1 H, C(4)_{H_{eq}}), 1.71–1.47 (m, 3 H, C(5)_{H_{ax}}, C(3)_{H_{eq}}, C(4)_{H_{ax}}), 1.34–1.23 (m, 1 H, C(3)_{H_{ax}}); ¹³C NMR (100.6 MHz, CDCl₃) 215.53 (C=O), 140.84 (*ipso*-Ph), 128.30 (*m*-Ph), 127.81 (*p*-Ph), 126.95 (*o*-Ph), 74.64 (CHOH), 57.35 (C(2)), 42.60 (C(6)), 30.76 (C(3)), 27.74 (C(5)), 24.63 (C(4)); IR (CHCl₃): 3536 (m), 3066 (m), 3033 (m), 2945 (s), 2904 (m), 2868 (m), 1697 (s), 1497 (m), 1450 (s), 1426 (m), 1400 (m), 1322 (m), 1312 (m), 1297 (m), 1226 (s), 1201 (s), 1191 (m), 1130 (s), 1101 (m), 1064 (m), 1041 (s), 1029 (m), 1016 (m), 846 (m), 777 (m), 731 (m), 724 (m), 707 (m); MS (EI, 70 eV) 204 (M⁺, 6), 186 (M⁺ – H₂O, 21), 106 (M⁺ – C₆H₁₀O, 40), 98 (M⁺ – C₇H₆O, 100), 70 (48), 55 (33); TLC *R*_f 0.24 (hexane/EtOAc, 3/1); [α]_D²⁴ –24.2 (*c* = 1.03, CHCl₃); HPLC *t*_R (2*R*,1′*S*)-6a 16.2 min (4.6%); *t*_R (2*S*,1′*R*)-6a 19.6 min (95.4%) (Chiracel OJ, 90/10 hexane/*i*-PrOH, 0.5 mL min^{–1}); HPLC *t*_R (2*S*,1′*S*)-6a 16.8 min (40.5%); *t*_R (2*R*,1′*R*)-6a 22.3 min (59.5%) (Chiracel OJ, 90/10

hexane/*i*-PrOH, 0.5 mL min⁻¹). Anal. Calcd for C₁₃H₁₆O₂ (204.27): C, 76.44; H, 7.90. Found: C, 76.45; H, 7.80.

General Procedure for Catalyzed Aldol Additions of **4 with Slow Addition of Aldehyde:** (–)-(2*R*,1′*S*)-2-(Hydroxyphenyl-methyl)cyclohexanone (*anti*-**6a**). Catalyst (*S,S*)-**7a** (37.6 mg, 0.1 mmol, 0.1 equiv) was dried under vacuum (0.05 mmHg) for 12 at rt, CH₂Cl₂ (5 mL) was added, and the solution was cooled to –75 °C (internal). Trichlorosilyl enolate **4** (200 μL, 1.1 mmol, 1.1 equiv) was added dropwise over 2 min. A solution of benzaldehyde (102.0 μL, 1.0 mmol) in CH₂Cl₂ (5 mL) was then added to the first solution, dropwise, via cannula over 45 min. During the addition, the temperature remained at –75 °C. The reaction mixture was stirred at –75 °C for 30 min, it was quickly poured into cold (0 °C) satd aq NaHCO₃ solution (10 mL), and the slurry was stirred for 15 min. The two-phase mixture was filtered through Celite, the phases were separated, and the aqueous phase was extracted with CH₂Cl₂ (3 × 50 mL). The organic phases were combined, dried over Na₂SO₄, filtered, and concentrated. The syn/anti ratio was determined by ¹H NMR (500 MHz) analysis to be 1/>50. The crude material was purified by column chromatography (SiO₂, hexane/EtOAc, 6/1) to give 2.4 mg of (–)-*syn*-**6a** as an oil and 189.8 mg (94% total) of (–)-*anti*-**6a** as a clear oil. Analytical Data for (–)-*syn*-**6a**: SFC *t*_R (2*S*,1′*S*)-**6a** 2.62 min (41.0%); *t*_R (2*R*,1′*R*)-**6a** 3.26

min (59.0%) (Chiralcel OJ, 150 bar, 40 °C, 6% CH₃OH in CO₂, 2.5 mL min⁻¹). Analytical Data for (–)-*anti*-**6a**: SFC *t*_R (2*S*,1′*R*)-**6a** 2.23 min (4.5%); *t*_R (2*R*,1′*S*)-**6a** 2.54 min (95.5%) (Chiralcel OJ, 150 bar, 40 °C, 6% CH₃OH in CO₂, 2.5 mL min⁻¹).

Acknowledgment. We are grateful to the National Science Foundation for generous financial support (CHE 0105205 and 0414440). S.M.P. thanks the Eastman-Kodak Co. for a graduate fellowship. X.S. thanks the University of Illinois for a graduate fellowship. Y.N. thanks the Ministry of Science and Education of Japan for a postdoctoral fellowship. We thank Mr. Bruce Williams for assistance in the design and construction of the RINMR apparatus and Dr. Martin Eastgate for helpful discussions.

Supporting Information Available: Detailed procedures for the preparation and characterization of phosphoramidate catalysts, aldolization experiments, nonlinear effect studies, and all kinetic (GC, ReactIR, and RINMR) experiments. This material is available free of charge via the Internet at <http://pubs.acs.org>.

JO060243V